MINERALOGICAL AND MICROBIAL CONTROLS ON IRON REDUCTION IN A CONTAMINATED AQUIFER-WETLAND SYSTEM

A Thesis

by

ANDREA MELISSA HOWSON

Submitted to the Office of Graduate Studies of
Texas A&M University
in partial fulfillment of the requirements for the degree of

MASTER OF SCIENCE

December 2010

Major Subject: Geology

MINERALOGICAL AND MICROBIAL CONTROLS ON IRON REDUCTION IN A CONTAMINATED AQUIFER-WETLAND SYSTEM

A Thesis

by

ANDREA MELISSA HOWSON

Submitted to the Office of Graduate Studies of
Texas A&M University
in partial fulfillment of the requirements for the degree of

MASTER OF SCIENCE

Approved by:

Chair of Committee,	Anne Raymond
Committee Members,	Jennifer McGuire
	John Morse
Head of Department,	Andreas Kronenberg

December 2010

Major Subject: Geology

ABSTRACT

Mineralogical and Microbial Controls on Iron Reduction in a Contaminated Aquifer-Wetland System. (December 2010)

Andrea Melissa Howson, B.S., Texas A&M University

Chair of Advisory Committee: Dr. Anne Raymond

Iron reduction is an important redox reaction in anaerobic environments for both biological and chemical cycling of elements such as carbon. However, the controls on the rate and extent of iron reduction are poorly understood and unlike other major terminal electron accepting processes, iron reduction has the added complexity that its oxidized form (ferric iron) exists primarily as one of several solid phases in environments with pH greater than 3. Thus, the distribution and form of ferric iron minerals are important controls on iron reduction in natural systems. For the first phase of this research a series of sequential chemical extractions was performed on a core taken from a landfill-leachate-contaminated wetland-aquifer system at the Norman Landfill, Norman, OK. The phases targeted by the sequential extractions consist of easily water soluble salts and ions present in the soil solution; weakly acid soluble iron (such as siderite and ankerite); easily reducible iron (such as ferrihydrite and lepidocrocite); moderately reducible iron (such as goethite, akageneite, and hematite); organically bound iron; magnetite; and pyrite. The second phase of this research involved creating *in situ* microcosm experiments that exposed native microbial communities to a test solution amended with 2-line ferrihydrite ($Fe_5HO_8 \cdot 4H_2O$), electron

donor (lactate and acetate), and a conservative tracer for a period of eleven days. The kinetics of iron reduction were then evaluated over time and the resulting changes in microbial community structure documented through DNA and RNA analysis.

Results document the spatial distribution of iron phases at the contaminated wetland-aquifer interface. Results of the sequential extractions indicate that ferrihydrite was present throughout the core. Accordingly, ferrihydrite was used in subsequent experiments on *in situ* microcosms to evaluate the kinetic controls on the microbial reduction of ferrihydrite. The results of these experiments show that microbial communities actively responded to the introduction of the amended ferrihydrite solution by increasing their community size and reducing ferrihydrite to an iron (II) phase in increasing amounts over an eleven day period.

DEDICATION

To my Husband, Jonathan Howson, my everything. To my sister, Dorinda, your belief in me means more than you will ever know. To my Mom and Dad, you gave me the foundation on which I stand.

Thank you all.

ACKNOWLEDGEMENTS

I would like to thank my previous committee chair, Dr. Jennifer McGuire; I have learned much through you and it is in big part because of you that I am where I am today. Thank you for seeing something in me and giving me a chance to work for you. I would also like to thank my current committee chair, Dr. Anne Raymond. It was a pleasure to get to know you and work with you. You gave me so much good life advice and I thank you deeply for that. Thanks also to my committee member, Dr. John Morse for being so accommodating and allowing me to work in your lab and use your facilities. I want to thank each of you for your guidance, your support and your willingness to help me find my way. In addition, I would like to thank Dr. Piers Chapman. You took this paper and helped me to make it better. Though I never had the opportunity to work with you, your thoughts and guidance at the end taught me a lot. Thank you for your time, your help, and your dedication. To all of you, your efforts are deeply appreciated. I cannot thank you enough from the bottom of my heart.

I would also like to acknowledge my colleagues, many of whom are now my good friends. A special thank you to my office mates, Dr. Susan Baez-Cazull, Dr. Tara Kneeshaw, and David Hansen. You were all constant and helpful guides throughout my masters work. My colleagues, Brandi Reese and Janie Lee, thank you for graciously allowing me in to your lab, showing me the ropes, and constantly being patient with me.

I would also like to thank the department faculty and staff for the help and support that they gave me. I would especially like to acknowledge the following people for their

constant help and the effort that they went to for me: Erik Smith, Ray Guillemette, Ryan Young, Steve Tran, Debbie Schorm, Gwen Tennell and Debra Stark.

In addition, I would like to recognize the United States Geological Survey (USGS). Specifically, I would like to thank Isabelle Cozzarelli, Mary Voytek, Julie Kirshtein, and Jason Masoner for allowing me to work with them on the Norman Landfill Project and for their help both in the field and in the lab. Allowing me to use your field site, and your efforts in the lab with the DNA and RNA analysis was essential to me. Thank you for your time and help. I would also like to extend thanks to the National Science Foundation for funding.

Lastly, I would like to thank Jonathan Howson, for your consistent help, your time that you gave up, the long hours of work and help that you gave to me. You worked tirelessly for me without complaint, and for that I thank you most of all.

TABLE OF CONTENTS

Page

LIST OF FIGURES

FIGURE Page

LIST OF TABLES

1. INTRODUCTION

A fundamental issue in understanding chemical fate and transport in natural systems is understanding the mineralogical and microbial controls on iron cycling. In contaminated systems, one of the main driving forces behind natural attenuation is the *reduction-oxidation cycle* or redox cycle. Redox processes are suggested to occur in a sequential pattern of redox zones dominated by terminal electron accepting processes (TEAPs) (Baun et al., 2003; Christensen et al., 2000; McGuire et al., 2002; McGuire et al., 2000; Scrow and Hicks, 2005; Vroblesky and Chapelle, 1994). Terminal electron acceptors (TEAs) are compounds that are accepted or utilized by microbes to obtain energy during the metabolism of an electron donor or carbon source. Studies have shown that through microbially mediated biological processes, as well as other processes such as physical and chemical cycles, natural attenuation of a contaminant plume can occur through sorption, dispersion, volatilization, dilution, abiotic degradation and biodegradation (Crapse et al., 2005; Wilson et al., 2004). Microbial communities are able to facilitate biodegradation of contaminants in freshwater systems through the use of the carbon cycle in conjunction with other cycles such as the sulfur cycle, iron cycle, nitrogen cycle, etc. In this study, the focus will be on the interactions of the carbon cycle with the iron cycle. The integration of these two cycles via the reduction that occurs through microbially mediated processes provides an important method by which contaminants are degraded.

This thesis follows the style of *Geochemica et Cosmochimica Acta.*

When a microbe reduces iron (III) in conjunction with a carbon source, the carbon becomes oxidized into CO_2, which is then utilized by the surrounding plants. Through this process, microbes are able to facilitate bioremediation of contaminated sites. Contaminated wetland-aquifer systems present complex interfaces that have a high potential for iron cycling. However, the spatial and temporal dynamics of iron reduction are not well understood. Fortunately, these types of systems are opportune for the study and observation of iron cycling.

It is known that iron redox processes play a highly important role in influencing the geochemistry of subsurface environments (Hyacinthe et al., 2006; Lovley, 1997). The process of reducing iron yields a large amount of energy; microbes harness that release of energy, resulting in microbially mediated iron reduction. However, some ferric iron phases provide a much higher energy yield than others, (Table 1). Accordingly, it is important to consider the redox potential of the different ferric iron phases, as it appears likely that phases with higher energy yields will be consumed first and more rapidly than other phases.

Table 1. Energy yield of iron oxide minerals.

Mineral Name	Formula	$\Delta G°$ (kJ mol^{-1})
Lepidocrocite	γ-FeOOH	-477.7
Goethite	α-FeOOH	-488.6
Ferrihydrite	FeOOH	-699
Maghemite	γ-Fe_2O_3	-711.14
Hematite	α-Fe_2O_3	-742.8
Magnetite	Fe_3O_4	-1012.6

(Cornell and Schwertmann, 2003)

However, the specific phases of ferric iron that are preferred by microbial colonies have yet to be studied within this system due to the many complexities associated with iron. These complexities include the wide variety of ferric iron phases existing at a pH greater than 3 (Thamdrup, 2000). For example, iron (III) may occur in phases of varying mineralogy and crystallinity. These differences between iron (III) phases can affect their chemical reactivity as well as the availability of iron phases to iron reducing microorganisms (Hyacinthe et al., 2006). An additional complexity is the ability of iron (III) to move from a solid state to a dissolved state upon reduction (Thamdrup, 2000). When ferrous iron becomes oxidized its initial product is iron (III), generally ferrihydrite (Thamdrup, 2000). Over time, ferrihydrite will change into a more stable crystalline form and will likely end up as goethite, hematite, or magnetite (Cornell and Schwertmann, 2003).

This project aims to discover where, vertically, the different phases of iron oxides are dominant. In a simple (homogeneous system), it is suspected that the most amorphous phases of ferric iron will be located near the surface sediments, while the more stable crystalline forms of ferric iron will be found deeper in the wetland sediments. It is also suspected that the more reduced iron forms (Fe II) will exist deeper in the core, in the anoxic layers. However, at the Norman Landfill Slough, heterogeneity in sediment type (silt, fine sand, coarse sand), and the presence of the leachate plume at depth may alter the ideal distribution of the iron phases with depth. The overall objective of this research is to understand the key mineralogical and microbiological controls on iron cycling in the linked wetland-aquifer system.

The goal of this research is to discover the spatial distribution with depth of a series of terminal electron accepting iron phases that may be utilized by microbial communities, as well as to understand the rate at which microbial communities are able to adapt and respond to the geochemical perturbation of ferrihydrite solution. This research has the potential to be used in numerical models to understand the overall rate at which a contaminant plume can be naturally attenuated.

There are two main approaches used to perform this research. The first is to analyze a core taken from the research site by performing sequential extractions, followed by Atomic Absorption analysis to evaluate the abundance of the predominant iron phases located in each of the different sections of the core. The second phase of this research is to investigate the microbial kinetics by which a common iron phase, ferrihydrite, is reduced.

2. STUDY SITE

The Norman Landfill research site in Norman, OK is a closed municipal landfill located near the Canadian River, which was in operation from the early 1920's until 1985. During this time, the landfill received unrestricted waste in two unlined landfill cells. In 1985 the cells of the landfill were closed with an earthen cap, and are now of particular interest due to a plume that has developed down-gradient from the landfill (Christenson et al., 1999). The plume contains elevated concentrations of dissolved organic carbon (DOC), chloride, ammonia, and methane (Christenson and Cozzarelli, 1999). An old channel of the Canadian river has created a wetland, which is also down-gradient from the landfill and overlies the plume (Figure 1). In addition to the plume and wetland, an aquifer exists a few feet below the surface of the wetland, creating a dynamic and unique interface. Biogeochemical cycling across this interface is the primary focus of this research.

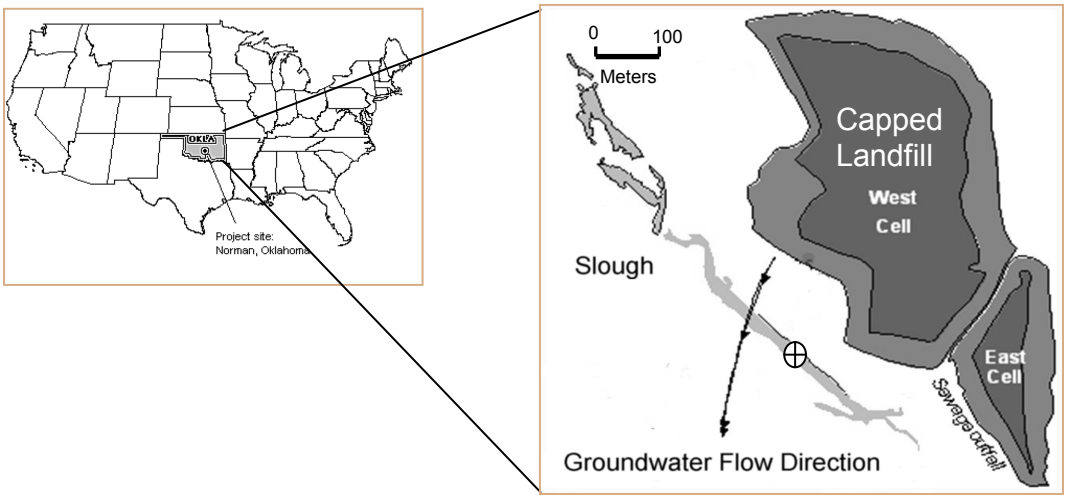

Figure 1. Map showing the study site location, Norman Landfill Research Site, Norman, OK, USA. Circle with cross hairs (right) represents actual location of study site.

3. PERFORM A SERIES OF SEQUENTIAL EXTRACTIONS ON SECTIONS OF A CORE FROM THE NORMAN LANDFILL RESEARCH SITE, NORMAN, OK

Iron reduction is an important redox reaction in anaerobic environments in terms of both biological and chemical cycling of elements such as carbon. However, the controls on the rate and extent of iron reduction are poorly understood. Unlike other major terminal electron accepting processes, iron reduction has the added complexity that its oxidized form (ferric iron) exists primarily as one of several solid phases in environments with pH greater than 3. Thus, the distribution and form of ferric iron minerals are important controls on iron reduction in natural systems.

Several studies have used sequential extractions as a method to evaluate the speciation of trace metals that exist in various sediments (Ahnstrom and Parker, 1999; Heron et al., 1994; Lovley and Phillips, 1986; Poulton and Canfield, 2005; Raiswell et al., 1993; Rapin et al., 1986; Sorensen, 1982; Stookey, 1970; Tessier et al., 1979; Tokalioglu et al., 2003; Van Bodegom et al., 2003). The procedure is among the most commonly used due to the ability to gather data about the origin, occurrence, and availability of trace metal phases being assessed within the sedimentary conditions of interest (Peltier et al., 2005; Tessier et al., 1979).

To execute phase 1 of this project, a series of sequential extractions was performed on a section of core removed from the wetland-aquifer interface. After analysis, these extractions served to indicate where, spatially, different phases of ferric iron exist in the core. These extractions also indicated, quantitatively, how much of each

phase is available. The exact phases extracted by each reagent are operationally defined. This is a limitation of sequential extractions in that most extractant reagents are unable to specify specific iron phases as perfectly as intended, and often other phases may also be extracted at the same time. The iron oxide phases that were targeted for each sequential extraction step in the experiment are listed in Table 2.

One of the main objectives of this study was to describe the iron phases that exist with depth in the wetland-aquifer system. Therefore, it is important to know the solid phase mineralogical make up of the soils of the column. Accordingly, each section of the column was subjected to XRD analysis to determine solid phase mineralogies with depth within the sediments of the wetland.

Table 2. Iron oxide phases targeted for each sequential extraction step.

Phase Targeted	Iron Oxide
Water	Easily soluble salts and ions present in soil
Exchangeable	Ion-Exchangeable Fe (II)
Weakly Acid Soluble	Siderite Ankerite
Easily Reduced	Ferrihydrite Lepidocrocite
Moderately Reducible	Maghemite Akageneite Magnetite
Organic	Organic matter
Iron Oxides	Goethite
Pyrite	Pyrite

3.1 METHODS

Task 1: Extract a Core From Wetland Sediments and Evaluate the Spatial Distribution of Iron Phase

A 76.2 X 1.76 cm tenite butyrate core liner was divided into six sections (each section had one port drilled prior to the coring), which were used to extract porewater from the cored sediments. The ports were located in the middle of each section at 10.16 cm intervals (Figure 2). Each port was covered with black electrical tape to prevent leakage.

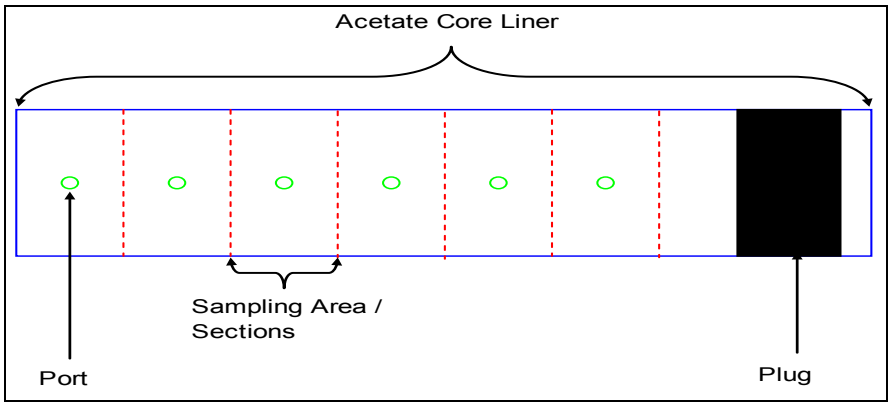

Figure 2. Schematic of core sections and port placement.

The core liner was hand-driven into the wetland sediments to a depth of approximately 76 cm. Coring took place in the subsurface of the wetland, as indicated in Figure 1. Upon retrieval, the ends of the core were immediately wrapped in a layer of saran wrap to maintain the anaerobic state of the core. The total length of sediment collected in the core was then measured and found to be 76.84 cm. The larger length occurred because of a small length of soil attached to and extending beyond the bottom

of the core liner. The core was then carried back to the work site where the electrical tape was removed and syringes were immediately inserted in to each port. The syringes were used to extract porewater from the sediment in the core. Samples were collected for the geochemical parameters summarized in Table 3. Preservation techniques for the anion samples involved using 10 µl formaldehyde stored at 4^{o}c. The ammonium and organic acid samples were preserved with flash freezing by being placed in a cooler containing dry ice. Cation samples were preserved with HCl and analyzed by capillary electrophoresis (Agilent Technologies, Wilmington, DE). Precision for capillary electrophoresis analyses is better than 0.1 mg/L. Trace metal grade concentrated HCl (Optima, 10 µl) and 0.5 ml of 2N zinc acetate was used to preserve the iron (II) and H_2S samples. The analysis for these samples was done using a Spectronic20D+ spectrophotometer (Thermo Spectronic, Rochester, NY), while in the field. Precision for iron (II) analyses were better than that of 0.1 mg/L and 0.001 mg/L for H_2S. Unfortunately, there was not enough porewater solution at each port within the core to collect a full suite of samples for each geochemical parameter. The results can be found in Appendix B.

After sample collection, the core was placed into an anaerobic glove bag filled with N_2 gas to prevent oxidation of the sediments. The core was split lengthwise and the sediment layers were described and measured. Sediment samples were collected from each section by removing 2 inches of sediment from either side of a port. Care was taken to not include any sediment that touched the inside wall of the core liner to ensure representative samples were obtained. The samples were placed into mason jars and

subsequently frozen (using dry ice) along with the core to maintain *in situ* conditions for further analysis.

Table 3. Summary of geochemical parameters collected from core.

Section	**Ammonium** NH_4^+	**Cations** Ca, Mg, Mn, Na	**Organic Acids** Lactate, Acetate, Propionate, Formate	**Anions** Cl^- SO_4^{2-} NO_3^-	**Iron** Fe^{2+}	**Sulfide** H_2S
1			X	X	X	X
2			X	X	X	X
3	X		X	X	X	X
4	X		X	X	X	X
5	X		X	X	X	X
6	X		X	X	X	X

As seen in Figure 3, the top layer of the core consists of organic sediments, the middle layer is a porous sand layer acting as shallow aquifer, and the bottom layer is composed of organic sediment. Because of the porous nature of the sand layer, oxygenated water is reintroduced during a recharge event. This allows the ferrous iron in this layer to become reoxidized; thereby, returning it to the more crystalline ferric iron state. This process should result in the sand layer having a higher abundance of crystalline ferric iron when compared to the other layers. The Munsell values for the sediment layers were also determined (Table 4).

Table 4. Munsell values for core.

Top of Core	Hue	Value/Chroma
Silt	10YR	4/3
Sand	10YR	5/3
Clay	10YR	3/3
Bottom of Core		

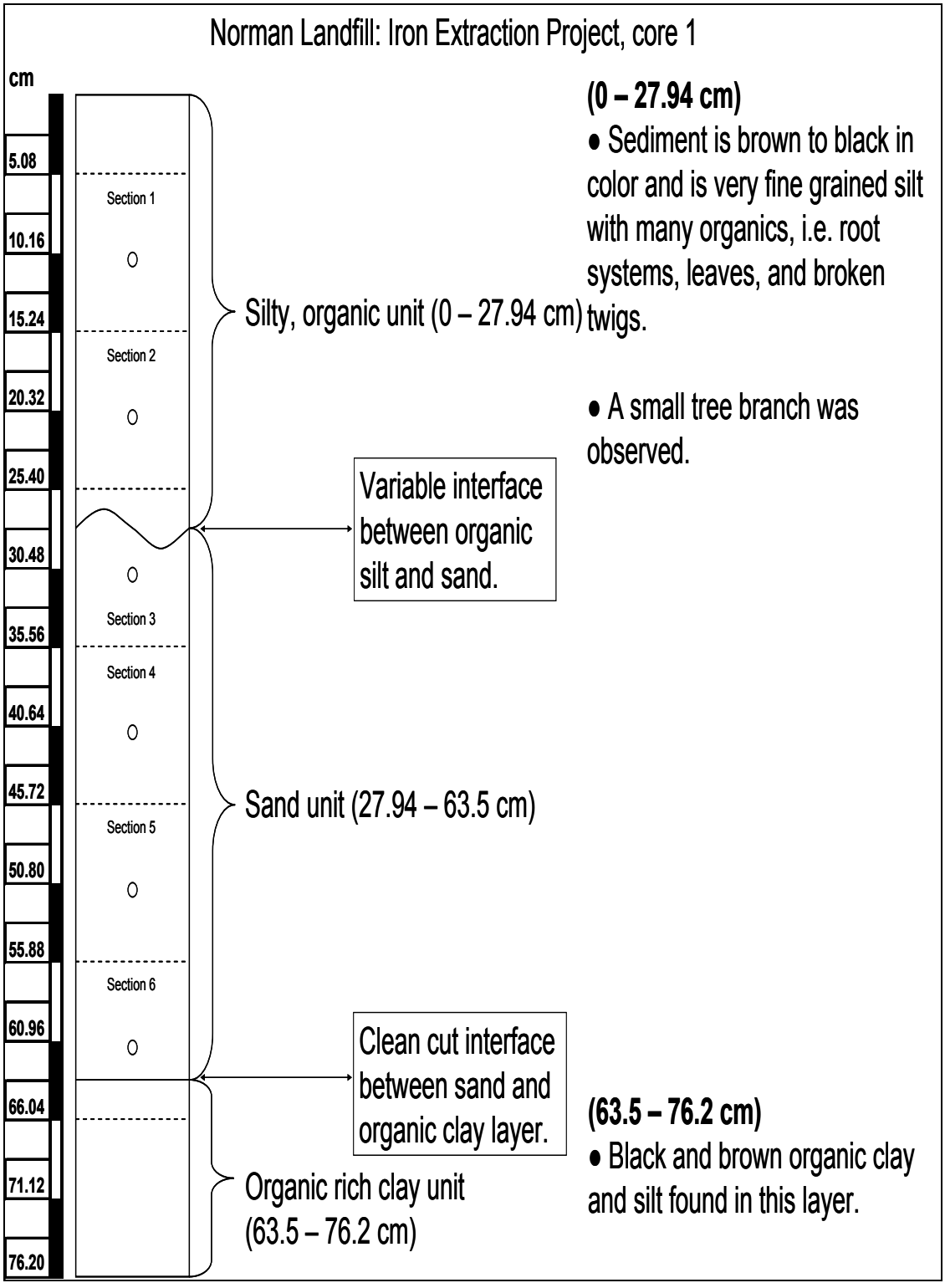

Figure 3. Schematic of core taken from site SI-102.

Task 2: Perform Sequential Extractions on the Six Sections of Sediment Sample Taken From the Core

The core was subsampled for extraction analysis in a glove bag filled with N2 gas as discussed above in Task 1. The sample was then homogenized inside a sterile Mason jar with a sterile spatula. Extractions were performed in triplicate for each section to get the best analysis possible. Thus, three sets of ten grams of each sample were weighed out and placed into each centrifuge sample tube (Figure 4). An outline of the following steps is located in Table 5.

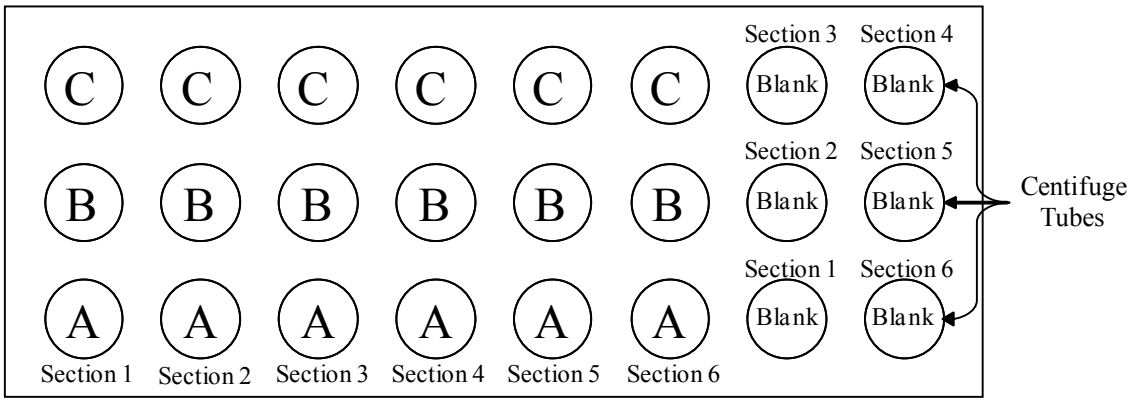

Figure 4. Aerial representation of the replicates, A, B, and C of each section, as well as the blank for each section.

Table 5. Breakdown of the different parameters for each fraction.

Experimental Procedure Information on Performance of Fractions

Step	Reagent	Sample Amount	Solution Make-up	Titration Reagent	pH Slope	Initial pH	Final pH	Reagent Added	Agitation Time/Level	Centrifuge Time/Level	Supernatent Collected
1	Water	10 G	Nanopure Water	N/A	N/A	N/A	N/A	25 mL	N/A	2 hr/40	17 mL
2	Exchangeable	10 G	1 M $MgCl_2$	$Na_2CO_3 \cdot H_2O$	99.6	5.6	7	25 mL	2 hr/10	2 hr/40	17 mL
3	Weakly Acid Soluble	10 G	1 M NaOAc	HOAc	98.5	8.47	4.5	25 mL	48 hr/10	2 hr/40	17 mL
4	Easily Reduced	10 G	1 M NH_2OH-HCl in 25% HOAc v/v	N/A	N/A	N/A	N/A	10 mL	48 hr/10	2 hr/40	17 mL
5	Moderately Reduced	10 G	50 g/L $Na_2O_4S_2$	0.35 M HOAc 0.2 M $Na_3C_6H_5O_7$	99.3	6.75	4.8	25 mL	2 hr/10	2 hr/40	17 mL
6	Organic	10 G	0.1 M $Na_4P_2O_7$	N/A	N/A	N/A	N/A	25 mL	18 hr/10	2 hr/40	17 mL
7	Amorphous Iron Oxides	10 G	0.2 M NH_4OAc / 0.17 M $H_2C_2O_4$	N/A	N/A	N/A	N/A	25 mL	6 hr/10	2 hr/40	17 mL
8	Pyrite AVS	5 G	cold 6N HCl + $SnCl_2$	N/A	N/A	N/A	N/A	60 mL	Digestion for 1 hr	N/A	60 mL
	Pyrite TRS	1 G	1 M $CrCl_3$ acidified to 0.5 N HCl	N/A	N/A	N/A	N/A	40 mL $CrCl_3$ 20 mL HCl 10 mL ethanol	Boil for 1 hr	N/A	60 mL

Step 1: Water – Soluble Iron

The first step in performing the series of sequential extractions requires looking at the type and abundance of iron that is removed simply by water. These iron types should be fully available for reduction by microbial colonies. However, they generally tend to be low in concentration (Van Bodegom et al., 2003). To extract this fraction, methods by Van Bodegum (2003) were used as follows. Each centrifuge tube had 25 mL of Nanopure water pipetted into it. A blank was made for each section that consisted of a centrifuge tube filled with 25 mL of Nanopure water. All of these processes were performed in a glove bag filled with inert N_2 gas (all steps were performed in an anaerobic glove bag to prevent the oxidation of iron (II) minerals present in the soil. Following the addition of the Nanopure water, each centrifuge tube was capped and centrifuged at 2000 rpm for 120 minutes.

For each extraction step hereafter, the following procedures were performed once the step was completed. After centrifugation, the samples were placed back in to the N_2 filled glove bag where the supernatant was extracted from the centrifuge tube via a syringe equipped with a 3 inch polyethylene tube at the tip. A 0.45 μm millipore syringe filter was used to filter the supernatant into 60 mL Nalgene HDPE sample bottles after first rinsing the filter with 2 drops of supernatant. The bottles were placed into the refrigerator to await further analysis to be performed on a Varian SpectrAA-200 (Varian, Inc. North America). Once all of the supernatant was extracted from each centrifuge tube, the residual fluid in the centrifuge tube was emptied into a waste beaker. The remaining sediment sample was rinsed with 10 mL of Nanopure water by hand-wrist

action shaker agitation for 20 minutes and then submitted to centrifugation for 2 hrs at 2000 rpm. The final water wash was discarded prior to the next step in the extraction sequence.

Step 2: Exchangeable Iron

Exchangeable iron, i.e. ferrous iron or iron (II), is the reduced form of ferric iron or iron (III). This is important because the amount of ion-exchangeable iron (II) will indicate if this wetland-aquifer interface is a redox zone (Schlottmann, 2000).

In order to discover the amount of ion-exchangeable iron (II), created in the wetland environment, an amended procedure from Poulton and Canfield (2005) was used. While the sediment samples were being thoroughly rinsed via centrifugation, a 600 mL solution of 1M magnesium chloride ($MgCl_2$) was created. Titration with sodium carbonate ($Na_2CO_3 \cdot H_2O$) was performed to achieve a pH of 7. The magnesium chloride solution (25 mL) was added to each sample after the removal of supernatant from the final Nanopure water rinse. The vials were then agitated for 2 hours at the maximum level in the Hand-Wrist Action Shaker agitator and subsequently centrifuged for 120 minutes at 2000 rpm.

Step 3: Weakly Acid Soluble Iron

The next step involved extraction of weakly acid soluble iron. A 600 mL, 1 M solution of sodium acetate (NaOAc) was prepared and the pH was lowered to 4.5 by titrating acetic acid (HOAc) into the sodium acetate solution (Poulton and Canfield,

2005). The final solution was then distributed into each vial in 25 mL aliquots. The vials were then placed into a static water bath for 49 hours at a temperature of roughly 50.0^{o} C. Subsequent agitation for 1 hour followed by centrifugation for 2 hrs occurred.

Step 4: Easily Reduced Iron

A solution of 1 M Hydroxylamine-HCl was made and placed into each centrifuge tube in 25 mL aliquots once the Nanopure water used to clean the sediment was removed from the vials (Poulton and Canfield, 2005). The vials were then shaken in the Hand-Wrist Action Shaker for 48 hours trailed by centrifugation for 2 hours.

Step 5: Moderately Reduced Iron

A solution of sodium dithionite ($Na_2O_4S_2$) was prepared and titrated to a pH of 4.8 with a solution of 0.35 M acetic acid and 0.2 M sodium citrate ($Na_3C_6H_5O_7$) following the methods of Poulton and Canfield (2005). Subsequently 25 mL of the solution was added to each vial post the removal of the waste water used to clean the sediments. The vials were then shaken in the Hand-Wrist Action Shaker for 2 hours trailed by centrifugation for 2 hours.

Step 6: Organically Bound Iron

A 600 mL solution of 0.1 M sodium pyrophosphate ($Na_4P_2O_7$) was created and distributed into each vial in 25 mL aliquots after the Nanopure water used to remove the previous reagent was removed (Weiss et al., 2004). The vials were shaken in the Hand-

Wrist Action Shaker for eighteen hours at level 10 followed by centrifugation for 2 hours and supernatant removal.

Step 7: Amorphous Iron Oxides

A 600 mL solution of 0.2 M ammonium oxalate ($(NH_4)_2C_2O_4.H_2O$) and 0.17 M oxalic acid ($H_2C_2O_4$) solution was prepared and distributed into each vial in 25 mL aliquots following the procedures performed by Poulton and Canfield (2005). This process was performed after the Nanopure water was removed from each vial and deposited into a waste beaker. The vials were then shaken in the Hand-Wrist Action Shaker for 6 hours at level 10 followed by centrifugation for 2 hours at level 40.

Step 8: Acid Volatile Sulfides (AVS) and Total Reduced Sulfides (TRS)

To perform the recovery of the acid volatile sulfides, a 5g sample of the original sediment was removed from each section of the core and digested in cold 6N hydrochloric acid (HCl) and tin chloride ($SnCl_2$) solution (5g $SnCl_2$ per 20 mL of 6N HCl) in an Erlenmeyer flask using the previously defined methodology of Canfield and Cornwell and Morse (Canfield et al., 1986; Cornwell and Morse, 1987). Each flask underwent digestion for one hour. Following the digestion, trapping vessels used to collect all of the evolved acid volatile sulfides were capped and placed in the refrigerator to await analysis on a Shimadzu UV1601 Spectrophotometer.

To begin the process of evolving the total reduced sulfides in the core, it was necessary to build a Jones Reductor column (Figure 5). The column was built following

the methodology of Kolthoff (Canfield et al., 1986; Kolthoff and Elving, 1993). The purpose of building the column was to reduce $CrCl_3$ as it passed through the column and interacted with the zinc that was used to fill the column. Once the $CrCl_3$ was reduced, it was utilized in conjunction with concentrated HCl and ethanol as the digestion reagent that reacted with the sediment samples to release H_2S. The procedure that was followed to perform this digestion was that of Canfield et al., (1986).

Final analysis of the TRS and AVS solutions was performed on the UV1601 Visible Spectrophotometer. These analyses were performed using the Cline Method, which was observed to be the most reliable methodology of those available (Reese et al., 2009).

Figure 5. Photograph showing the Jones Reductor Column with $CrCl_3$ undergoing reduction (turning from a shade of dark forest green to the bright blue as seen above).

4. EVALUATION OF NATIVE MICROBIAL COMMUNITIES RESPONSE TO GEOCHEMICAL PERTURBATIONS

Microorganisms play a fundamentally important role in the biogeochemical cycling of iron in groundwater systems by utilizing available electron donors and acceptors for anaerobic respiration. Often, subsurface systems can experience influxes of electron acceptors and donors due to changes in the hydrologic conditions of the system. However, when a system changes and the subsurface solution becomes perturbed with an electron acceptor, little is known about how the native microbial communities respond to this influx. Furthermore, little is known about the initial framework of the microbial community. This is an important attribute as it is necessary to understand the initial structure of the microbial community in order to understand how the community changes once a perturbation is introduced. One reason why this has yet to be studied is because no experimental apparatus has been devised that will allow an *in situ* test to occur to observe the outcome of a community's response to a perturbation in its native environment. To gain a better understanding of a native microbial community's response to an influx of iron oxide rich solution, an enclosed microbial community was exposed to a test solution amended with ferrihydrite as an electron acceptor, and lactate and acetate as electron donors. The testing process for this experiment used an apparatus called a Native Organism Geochemical Experimentation Enclosure, or NOGEE, designed and fabricated by Erik Smith under the direction of Dr. Jennifer McGuire (TAMU). Through the use of the NOGEE the rate at which the

microbial community was able to reduce the ferrihydrite was studied, and the initial and final microbial community makeup was analyzed using DNA and RNA genetic analysis.

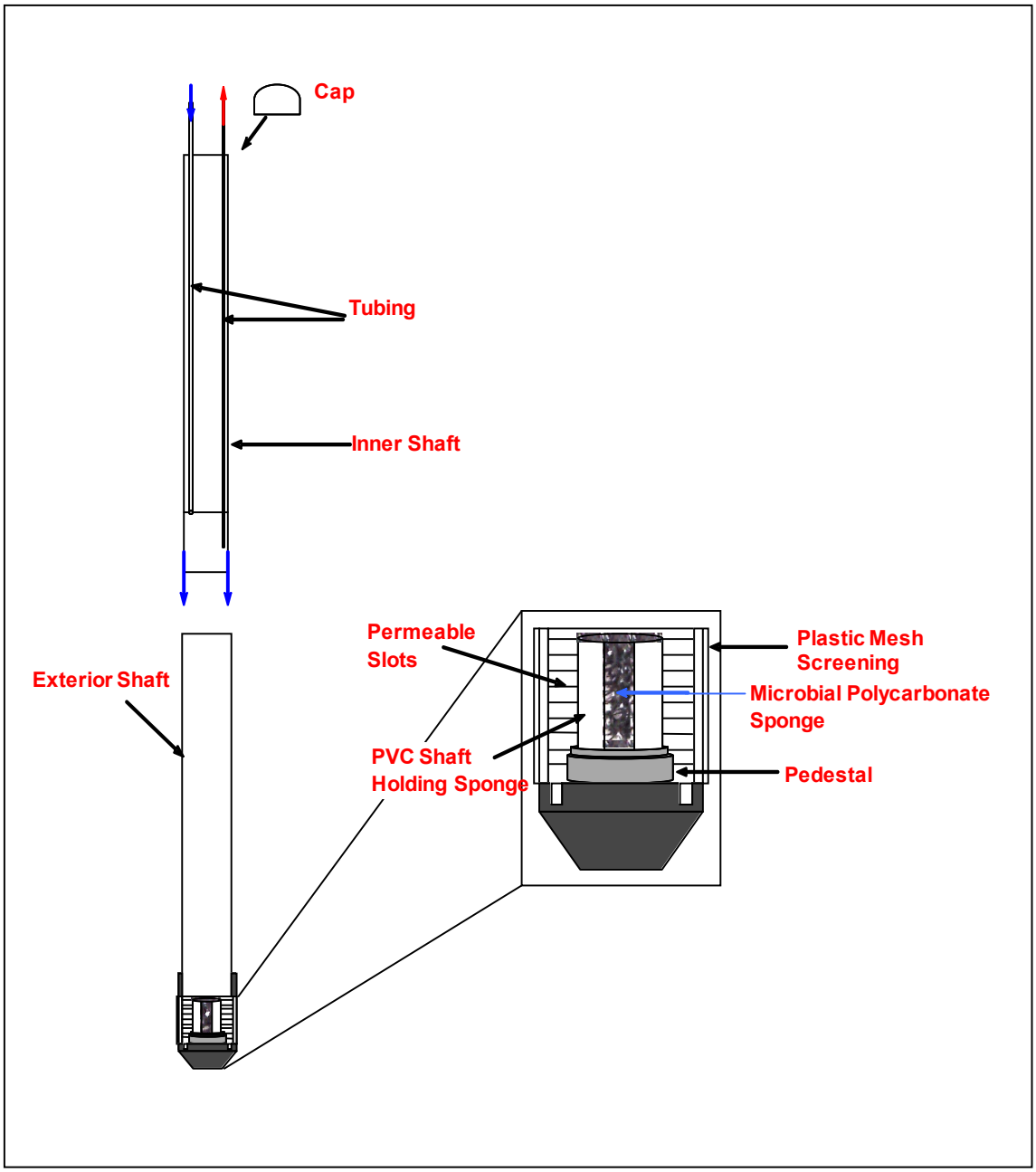

Figure 6. Depiction of NOGEE broken into two sections.

4.1 METHODS

Task 1: Fabrication of NOGEEs (Performed by Erik Smith) to Allow Microbial Communities to Establish a Colony, and be Subjected to Geochemical Perturbations

The latest version of the Native Organism Geochemical Experimental Enclosure (NOGEE) consists of a core compartment (5.33 cm W X 5.72 cm H) that is constructed from type 1 PVC. The core compartment contains a chemically inert polyethylene sponge located inside of a shaft of PVC that is glued to the pedestal at the base of the core compartment (Figures 6 and 7). The perimeter of the NOGEE is slotted so that water may pass in and out of the NOGEE, allowing the sponge to become colonized with microbes. To prevent sediment from entering through these slots, the circumference of the NOGEE is covered with a plastic mesh screening. The core compartment of the NOGEE was attached to a PVC pipe (5.33 cm W X 1.52 m H) that extended through the wetland sediment to the surface of the water. Contained inside the PVC pipe is another PVC pipe of smaller dimensions that is secured over the shaft containing the sponge. This pipe closes off the sponge, preventing the flow of wetland water from passing through the outer perimeter of the NOGEE and entering into the area where the sponge is in repose. The inner shaft was fitted with two tubes; one (Figures 6 and 7) allowed the introduction of amended test solutions into the enclosed chamber, and the other served to remove all fixed solutions from the chamber after a regulated number of days.

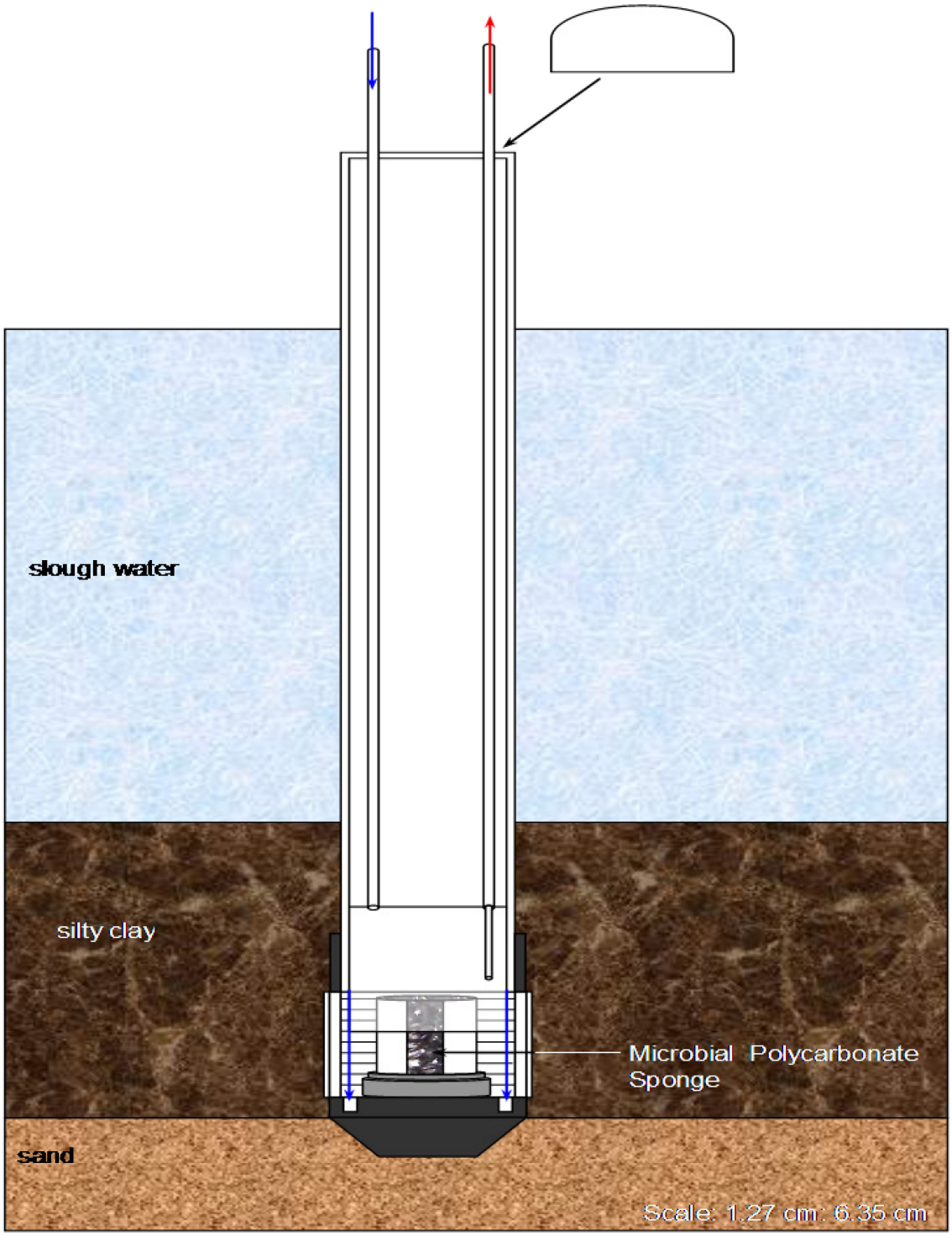

Figure 7. Diagram of NOGEE design during colonization stage.

When the NOGEEs were deployed, they were implanted completely through the silty clay layer until they were seated just past the surface of the sand (aquifer) layer (Figure 7).

Task 2: Prepare Ferrihydrite to Use in Amended Test Solution for NOGEES

Prior to performing field research, 2-line ferrihydrite was made following the original methodology of Schwertmann and Cornell (2000) with slight amendments made by Raven et al., (1998) (Raven et al., 1998; Schwertmann and Cornell, 2000). The different phases of ferrihydrite are characterized (in name) by the number of XRD peaks they possess (Schwertmann and Cornell, 2000). In addition, the number of peaks correlates to the crystallinity of the ferrihydrite, i.e. more peaks result in a more crystalline form of ferrihydrite. Therefore, the ferrihydrite made for this experiment only had two XRD peaks at a d-spacing of 2.4 and 1.5 Å, as shown in the Figure on page 29, and was the most amorphous form of ferrihydrite. The d-spacing corresponds to the x-axis (º2θ) through Bragg's Law, Equation 1.

Equation 1.

$$n\lambda = 2d\sin\theta$$

where n is an integer representing the atomic layer of the mineral where diffraction has occured, λ is the wavelength of the incident X-ray beam (λ = 1.0 Å), d is the interatomic spacing in angstroms and θ is the diffraction angle. Each mineral has its own set of

characterizing d values and related intensities. For 2-line ferrihydrite the 2θ values that correspond to the d-spacing values of 2.4 and 1.5 Å are 37 and 62, respectively.

The method to make the 2-line ferrihydrite began with making a 500 mL solution of 0.2 M $Fe(NO_3)_3 \cdot 9H_2O$ in a volumetric flask, which was then emptied into a 1L Nalgene stock bottle and placed onto a stir plate. While the solution underwent vigorous stirring, 276 mL of 1 M KOH was added to the solution. The KOH was added at a fixed rate of roughly 50mL/min from 100 mL burette. With the final 10 mL of KOH added dropwise, the pH of the solution was titrated, using a burette, to 7.50. After reaching the desired pH, the solution was left alone for thirty minutes while still maintaining a vigorous stirring to assure complete mixture. This step was performed to ensure that the pH of the solution was at equilibrium. Following the equilibration of the pH, the solution of ferrihydrite was divided into four 250 mL Nalgene stock bottles. Nanopure water was added to each bottle to wash the suspension as well as to make them all of equal weight. The bottles were then centrifuged at 2000 rpm for two hours. After centrifugation, the supernatant was decanted and each bottle was refilled with fresh Nanopure water, hand agitated, and placed on a vortex to assure the pellet was broken up and thoroughly mixed with the Nanopure water. The new solution was then centrifuged again. This process was repeated 4 more times. The purpose of this process was to rinse the congealed ferrihydrite of any nitrate analyte remaining in the solution. After the last two rounds of centrifugation, a CheMetrics Nitrate 1 VacuVial was popped to confirm the removal of the nitrate. Once the nitrate level was below the limit of detection, the ferrihydrite contents of the four bottles were placed into one 250 mL bottle which was

centrifuged one more time to remove all ferrihydrite particles from suspension in the Nanopure water. Before placing the sample in the refrigerator at 2^{o} C as suggested by Raven et al., (1998), a small portion of ferrihydrite was then removed from the bottle and freeze dried. This process was performed to prepare the ferrihydrite for powder analysis on the X-ray emission microscopy Electron Microscope Cameca SX50 as well as the X-ray Diffraction Spectrometer (XRD). The X-ray emission microscopy analysis was performed under the direction or Dr. Ray Guillemette from Geology & Geophysics, TAMU. These analyses were used to confirm the identity and purity of the 2-line ferrihydrite. Due to a malfunction in the X-ray emission microscopy Electron Microscope Cameca SX50, a qualitative analysis of ferrihydrite was unable to be performed. However, previous analyses of ferrihydrite samples using the same methodology had been performed by Susan Báez Cazull. Those analyses were used in comparison, quantitatively, to the sample of interest. These comparisons were within numbers expected of previous ferrihydrite data, and thus it was concluded that the sample was in fact ferrihydrite. Figure 8 displays the results found from the XRD analysis, which matches the XRD analysis that was given by (Schwertmann and Cornell, 2000).

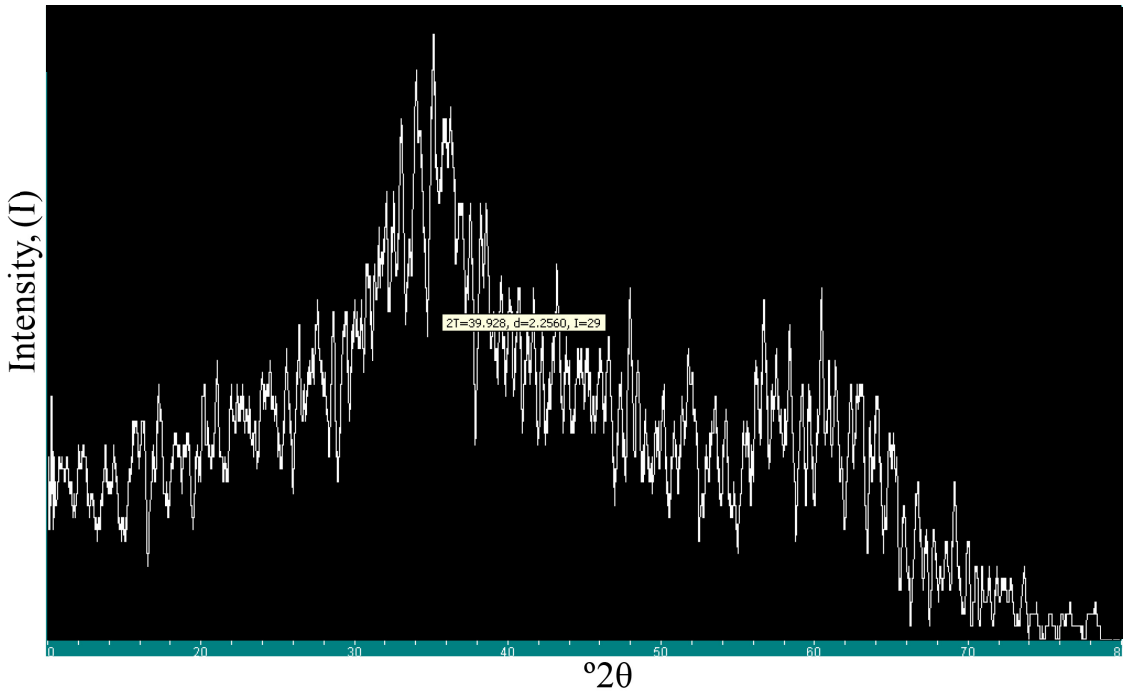

Figure 8. XRD analysis of ferrihydrite. X-axis scale is in º2θ, Y-axis is in intensity (I).

Task 3: Perform Experiments Introducing Amended Test Solution into Each NOGEE and Evaluate the Microbial Community's Response to the Geochemical Perturbations

Six weeks prior to performing field research, the NOGEEs were pounded into the wetland to allow a sufficient incubation period. Along with the NOGEEs, six blank wells (D1-D6), similar in style to drive point wells and containing only sponges, were driven into the ground (Figure 9). The blank wells consisted of a PVC pipe connected to a permeable drive chamber containing a chemically inert polycarbonate sponge (Figure 10). The blank wells served the purpose of allowing DNA analysis to be performed on the microbial communities without the introduction of geochemical perturbations. Before removing the blank wells from the wetland, wetland water contained in the internal chamber was removed from each well and sampled for the geochemical parameters. A peristaltic pump was used to remove this water. The geochemical parameters collected for each blank included sulfide, iron, anions, cations, organic acids, ammonium, alkalinity, methane and DOC. This data can be found in Appendix B.

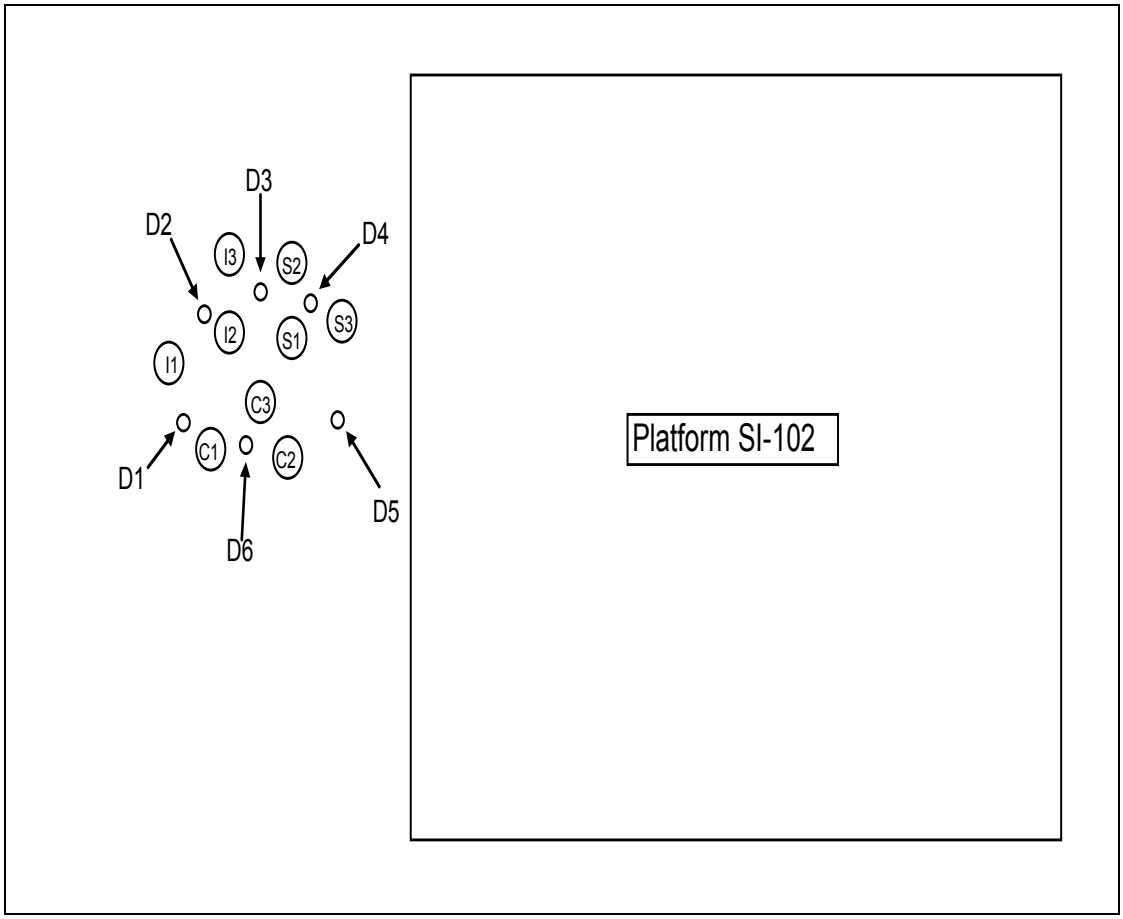

Figure 9. Actual arrangement of NOGEEs in the field. Dimensions of the platform were roughly 1.52 m L X 1.21 m W. NOGEEs were 5.08 cm in diameter and were spaced in a circular arrangement, approximately 0.46 m in diameter. The spacing between the NOGEEs was roughly 6.35 cm. The Dummy NOGEEs were 1.27 cm in diameter and were interspersed between the larger NOGGEs as seen above.

The first step in beginning the experimentation was to find a well at the sand layer (Figure 7) with low sulfate concentrations and an ample flow rate. Multi-level sampler (MLS) 38-6 (Figure 10) was found to have a copious source of groundwater for producing the test solutions that would be used throughout the experiment. Dissolved oxygen, pH, conductivity, temperature, and redox potential were measured on the

groundwater extracted from MLS 38-6 using a 600 XLM YSI Hydrodata multiparameter.

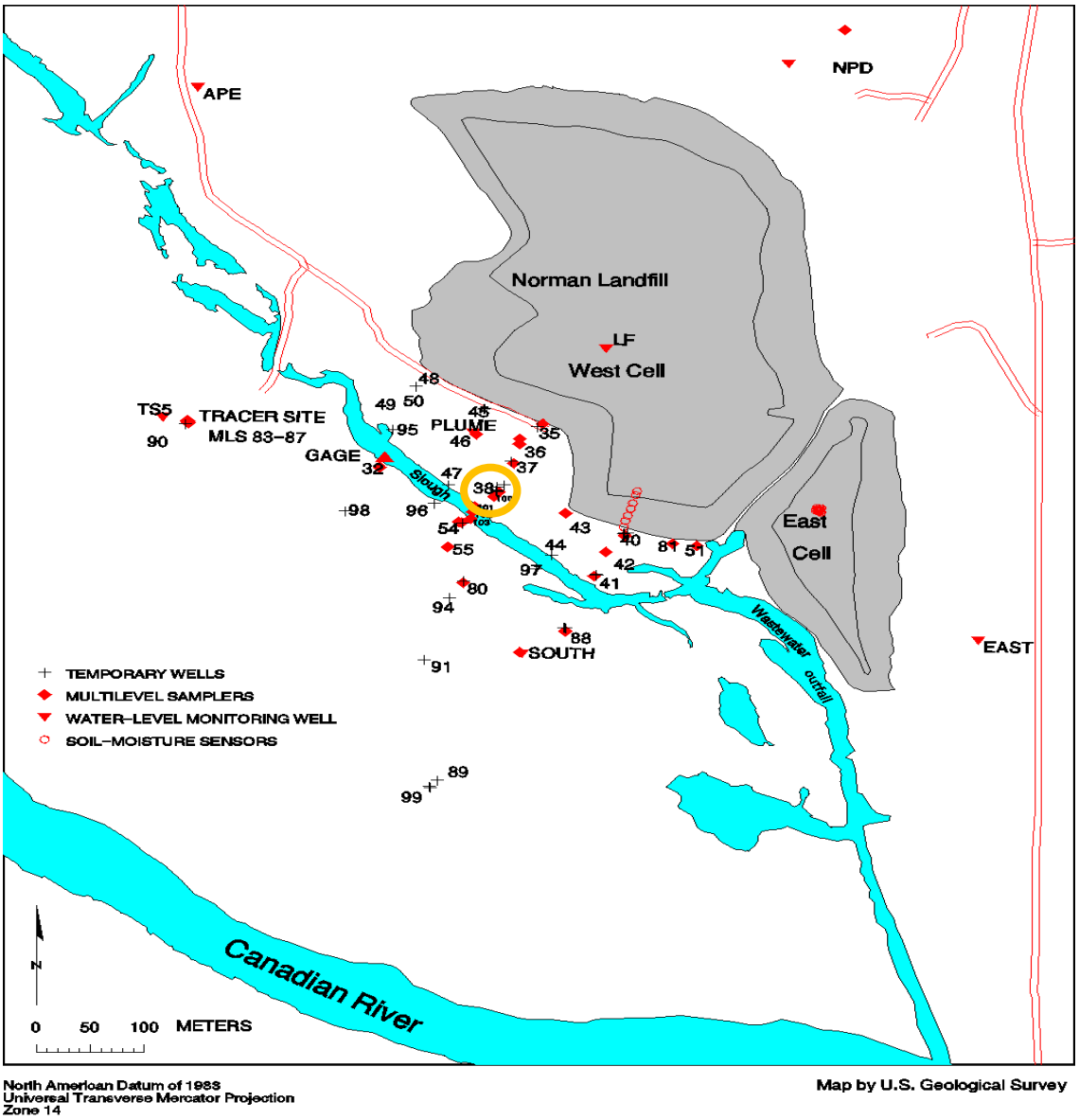

Figure 10. Layout of the different collection sites located at the Norman Landfill Research site. MLS 38, highlighted with a circle, is the sampling well of interest for this research project.

Creating the Amended Solution

An amber bottle, used as the mixing chamber for the amended solution, was placed in an ice-filled cooler to preserve the subsurface temperatures of the groundwater. Both the cooler and the amber bottle were then filled with argon gas to displace any oxygen, thereby preventing any oxidative processes. Once sufficiently filled with argon gas, the amber bottle was filled with 3L of groundwater pumped from MLS 38-6. Acetate (60 mg/L) and lactate (300 µl) were added to the solution as electron donors. In addition, bromide (100 mg/L) and ferrihydrite (130 mg/L) were added to the solution to act as a conservative tracer and electron donor, respectively. The sulfide NOGEEs utilized the same mixture, only exchanging 100 mg/L sulfate for the ferrihydrite. For the control NOGEEs, a test solution consisting of only groundwater and bromide was made. Once all of the amendments were added to the test solution, the amended solution was inverted multiple times for homogenization. Initial test solution (ITS) samples were taken to analyze for geochemical parameters. Finally, the amended solution was transferred into a tedlar gasbag to be pumped later into the NOGEE.

Addition of Amended Solution to NOGEEs

To prepare the NOGEEs for the addition of test solution the inner pipe (Figure 7) was lowered into position, completely sealing off the inner chamber. This process was operationally defined as seating. Each of the NOGEEs was seated by hand, meaning the inner PVC pipe was driven down over the internal chamber to seal off the compartment (Figure 6). In total, six NOGEEs were seated, two for each control (C), iron (I), and sulfate (S) test. The remaining three NOGEEs were pulled from the wetland, their sponges removed, and preserved on dry ice for DNA testing. Once the NOGEEs were securely seated, the outlet tube was connected to the 6-channel peristaltic pump tubing while the inlet tube was attached to a tedlar bag filled with argon gas, to prevent any oxygen from entering the system while fluids were being removed. The peristaltic pump was activated and 6 mL of solution was removed to clear the tubing of any oxygen-contaminated fluid. Subsequently, a clean syringe and filter were made ready and samples of the groundwater solution that became trapped in the internal chamber of the seated NOGEE were taken for geochemical analyses. This procedure was followed again at a later time when the incubated test solution was removed from the NOGEE.

The addition of the amended test solutions occurred by connecting the tedlar gasbag containing the test solution to the inlet tubing of the NOGEE via a 6-channel peristaltic pump. The amended test solution was pumped into the NOGEE until 100 mL of solution was expelled from the outlet tube. Once the NOGEE was sufficiently filled with the amended test solution the inlet and outlet tubing were folded over and taped closed to prevent any oxygen from entering the tubing.

The process outlined occurred five times in approximate 48-hour increments, over a period of eleven days. Additional test solution was added approximately every 48 hours to ensure that the microbial community never ran out of electron donors or acceptors to utilize in their redox processes. The purpose of performing this research was to see how the microbial community in each NOGEE would respond to the addition of a geochemically perturbed solution. The polycarbonate sponges contained in the internal chamber of each NOGEE were extracted and preserved at the end of the experiment for DNA analysis of geobacter (a proxy for Fe-reducers), to determine how the microbial community within each NOGEE reacted to the addition of the ferrihydrite amended test solution. Mary Voytek and her lab group performed the DNA and RNA analysis at the USGS in Reston, Virginia.

5. RESULTS AND DISCUSSION

5.1 SEQUENTIAL EXTRACTIONS OF IRON PHASES

Figure 11 is a graphical representation of the data contained in Table 6; which displays the concentration in parts per million (ppm) and types of iron (III) phases in each section of the extracted soil column. As seen in Figure 11, the total concentration of iron (III) in each section varied greatly due to the type of soil contained within it. A detailed schematic of the core, descriptions and vertical placement of the soil layers, and the vertical location of each section is illustrated in Figure 3. Due to the vast difference in concentration of iron (III) in each section, which ranged from 2144 ppm in Section 6 down to 201 ppm in Section 5, Figure 12 was included. Figure 12 shows the percent total concentration of each iron (III) phase in a section based on the total concentration of iron (III) in the given section, and indicates which section(s) contained the largest percentage of each iron (III) phase.

The results from the sequential extractions indicate that iron (III) phases vary dramatically with depth within the wetland. This is largely due to the vertical layering of the soil. Sections 1 – 3 are composed of fine grained silt with many organics and have high concentrations of iron (III). Roden and Wetzel (1996) discovered similar trends in the distribution of total iron (III) in the organic upper layers of a wetland system. Sections 4 and 5, Figure 11, are composed of mainly coarse-grained sand and contain the smallest concentration of total iron (III) phases. These two sections are contained within the sand layer, which contributes freshwater recharge to the system and

acts as a shallow aquifer. Baez-Cazull (2007) hypothesized that the shallow aquifer was connected hydraulically to the surface wetland. The low iron (II) found in the surface water, (Baez-Cazull, 2007), coupled with the low organic matter in found this layer may contribute to the low concentration of total iron (III) phases discovered in Sections 4 and 5. Section 6 is composed of organic rich clay and has the highest concentration of iron (III) phases.

Table 6. Summary of data results from sequential extraction experiment.

	Water Soluble	Easily Exchangeable	Weakly Acid Soluble	Easily Reducible	Moderately Reducible	Organic	Iron Oxides	AVS	TRS	**Total Concentration of Iron extracted (ppm)**
Section 1	0.7	0.7	910.0	160.0	186.7	23.3	36.0	37.23	15.77	1370.40
Section 2	0.4	0.0	950.0	296.7	403.3	49.0	63.7	47.30	13.64	1824.05
Section 3	0.5	0.0	490.0	176.7	326.7	436.7	123.3	200.39	48.07	1802.26
Section 4	1.5	0.0	33.7	35.7	113.3	17.7	42.0	0.00	36.57	280.41
Section 5	0.0	0.0	35.0	21.0	75.0	10.3	12.0	48.23	0.00	201.60
Section 6	0.2	0.0	760.0	106.7	496.7	196.7	416.7	120.28	47.49	2144.60

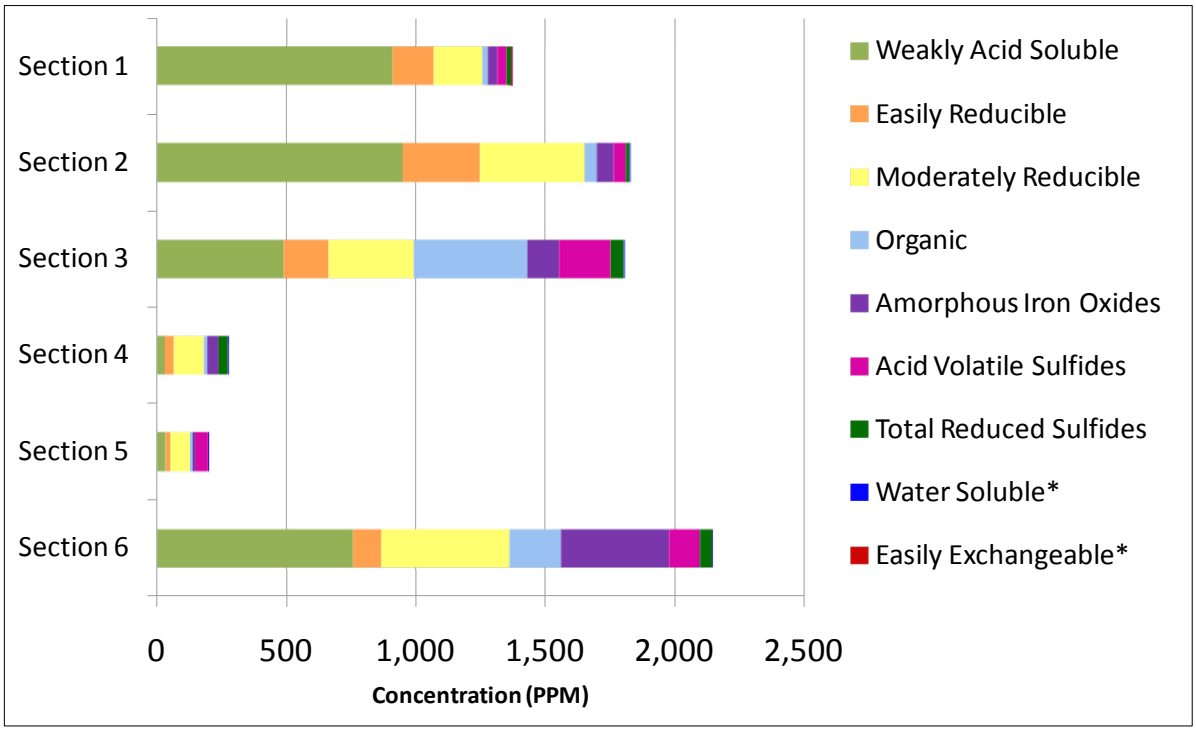

Figure 11. Concentration (ppm) results of sequential extractions displayed with depth. Section 1 represents the sediment-water interface. Data are presented in parts per million (ppm) of iron (III) phases extracted for each section. Asterisks (*) represent concentrations that are so minute they are unable to be seen in the graph above.

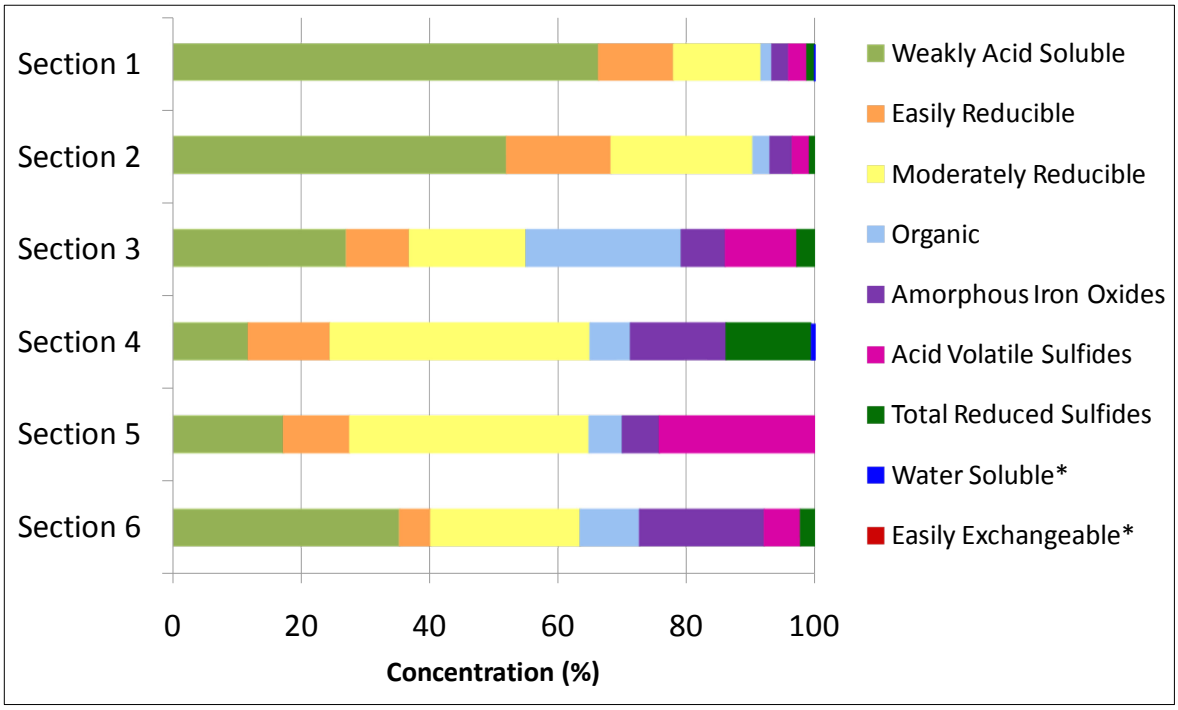

Figure 12. Percentage of total concentration results of sequential extractions displayed with depth. Data are shown in percentage of total concentration of iron (III) phases extracted for each section. Asterisks (*) represent concentrations that are so minute they are unable to be seen in the graph above.

The most abundant iron (III) phase throughout the core was weakly acid soluble, which include iron carbonates such as siderite and ankerite. This iron (III) phase composed 41.7% of the total iron (III) in all sections. The weakly acid soluble forms of iron are the most abundant phase in core sections composed entirely or partially of organic rich layers (sections 1-3, 6). These organic rich layers have calcium carbonate shells (snails, ostracods and bivalves; Welsh, 2007), as well as a high carbon content that can contribute to the formation of ankerite and siderite, which are iron carbonates. The second most abundant iron (III) phase in the core was moderately reducible, which composed 21.01% for the total iron (III) in all sections. Moderately reducible iron oxides constitute the dominant percentage in the coarse sand layer (sections 4 and 5; Figures 3 and 12). The influx of more oxygenated, anaerobic water into the sand layer via the aquifer engenders the possibility that sections 4 and 5 were more abundantly filled with the moderately reducible iron oxide phases due to the coupling of dissolved oxygen with any existing reduced iron. The least abundant iron oxide phases were the water soluble and easily exchangeable phases, with 0.04 % and 0.009% of the total iron (III) in all sections, respectively. Because of these low concentrations, these iron phases are indiscernible in Figures 11 and 12.

It was hypothesized that easily reducible iron (III) phases would be a dominant iron oxide phase utilized by iron-reducing bacteria at the sediment-water interface section of the core as well as an important iron oxide phase throughout the core. Larsen and Postma (2001) found that easily reducible iron (III) phases were the dominant terminal electron accepting iron phases. In a later study, Bonneville et al., (2004)

concluded that other variables such as surface area, crystallinity, and impurity content, affected the preferential order in which iron reducing bacteria selected iron (III) phases for reduction. The research conducted in this study showed that easily reducible iron (III) phases were present in all sections and constituted the third largest percentage (10.4%) of iron (III) phases (Table 6). Easily reducible iron (III) phases were an important electron accepting phase; however, most likely not the dominant terminal electron accepting iron phases in the wetland-aquifer system.

Acid volatile sulfides (AVS) and total reduced sulfides (TRS) were analyzed using the Cline Method on a UV spectrophotometer. The results indicated that AVS and TRS occurred in most sections of the soil column, as shown in Table 6. AVS was found in silt sections (sections 1, 3) and in the lower sand layer (5) as shown in Figure 11; with no detectable AVS presence found in the upper coarse sand layer (section 4). The largest concentration of AVS was contained at the bottom of the upper silt layer in section 3 (200.39 ppm). Detectible concentrations of TRS were found in silt sections (1, 3, and 6) and in the upper coarse sand layer (section 4) as displayed in Figure 11. The lower coarse sand layer (Section 5) contained no TRS. The largest amount of TRS (48.07 pm) was found in Section 3.

The validity of the acquired results for both the AVS and TRS phases are questionable. This is due to the late discovery that the samples needed to be titrated with HCl acid prior to analysis on the spectrophotometer to remove suspended particles. The original soil column samples had degraded past the point of yielding usable data upon

discovery of the missed step. Because of this, no accurate data for the concentrations of either AVS or TRS could be obtained.

The qualitative findings from the XRD analysis (Table 7) correspond reasonably well to the quantitative results determined through sequential extractions shown in Figures 11 and 12. Comparing the results from the two methods, it appears that the sequential extractions were able to positively identify all iron phases (e.g. water soluble, easily exchangeable, weakly acid soluble, etc.) present within each section of the core; however, was not able to identify the specific iron (III) minerals present within each phase (e.g ankerite, siderite, hematite, etc.). The XRD analysis, on the other hand, was able to positively identify several specific iron (III) minerals present within each section of the core, but was not able to identify an iron (III) mineral that corresponded to each iron (III) phase (Figures 11 and 12, Tables 6 and 7). The results from the XRD; however, more accurately identify the individual minerals present within each iron (III) phase for a given section.

When analyzing the data from the XRD, there were two classifications of minerals found: minerals "definitely present" and minerals "possibly present" (Table 7). Minerals that were "definitely present" matched all peaks from the XRD profile graph, and minerals that were "possibly present" matched at least the three strongest peaks, but not all peaks. The XRD profiles for each section and peaks for each mineral can be found in Appendix A.

Table 7. Qualitative findings of XRD results. Peaks corresponding to each mineral species are located in Appendix B.

	Definitely Present	Possibly Present
SECTION 1	Maghemite (Moderately Reducible) Goethite (Iron Oxides)	Hematite (Iron Oxides) Ferrihydrite (Easily Reduced) Feroxyhyte (Easily Reduced)
SECTION 2	Maghemite (Moderately Reducible)	Feroxyhyte (Easily Reduced)
SECTION 3	Magnetite (Moderately Reducible) Ferrihydrite (Easily Reduced) Ankerite (Weakly Acid Soluble)	Feroxyhyte (Easily Reduced)
SECTION 4	Hematite (Iron Oxides) Maghemite (Iron Oxides)	Ferrihydrite (Easily Reduced)
SECTION 5	Ferrihydrite (Easily Reduced)	
SECTION 6	Magnetite (Moderately Reducible) Ferrihydrite (Easily Reduced) Feroxyhyte (Easily Reduced) Ankerite (Weakly Acid Soluble)	Maghemite (Moderately Reducible)

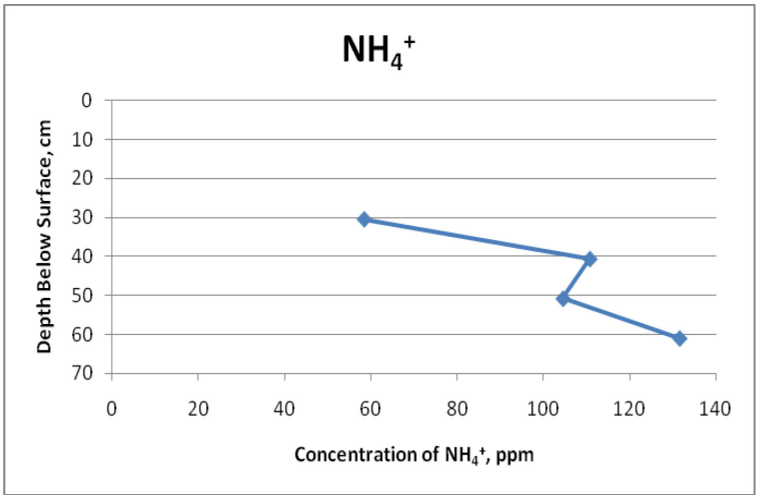

Figure 13. Depth-concentration profile for ammonium.

Ammonium

The ammonium-iron redox cycle has recently been found to constitute an important cycle in bioremediation processes (Chapelle 2001). Ammonium originates in the soil as a result of microbial decomposition of organic acids (Schlesinger 1997). Once released into the soil it can be affected by a variety of processes, such as uptake by plants, microbial immobilization (Schlesinger 1997), oxidation by microbes (Weber 2006), or reduction by microbes (Clement et al., 2005 and Weber 2006). Clement et al. (2005) studied the relationship between ammonium and iron (III) and found that ammonium is coupled to the reduction of iron (III). Their findings showed that iron (III) would become reduced to iron (II) while ammonium became oxidized to nitrite, (Equation 2).

Equation 2.

$$NH_4^+ + 6\ FeOOH + 10H^+ \rightarrow NO_2^- + 6\ Fe_2^+ + 10\ H_2O$$

However, Li et al., (1988) and Weber et al., (2006b) found that ammonium ultimately became oxidized to a final product of nitrate. In addition to this processes, the reverse processes has also been found to be successfully achieved by microbes (Weber et al., 2006a; Weber et al., 2006b). Whereby, microbes are able to reduce nitrate to ammonium in conjunction with the oxidation of iron (II) to iron (III).

Due to a limited supply of porewater solution available in the upper portion of the core, ammonium was not measured in sections 1 and 2 (Figure 13). Despite the lack of samples, it can be concluded from previous studies (Báez-Cazull et al., 2007; Cozzarelli et al., 2000) that ammonium would be present in these two sections from both active microbial cycling of wetland organic matter and through transport from the landfill leachate plume. The high levels of ammonium discovered in Sections 3 – 6 of the soil column are consistent with nitrate reduction, yet nitrate levels throughout the soil column were below detection except in Section 1, Figure 14b. Sections 3 through 6 of the core show a general increase in ammonium with depth. Three alternatives are available that could explain this occurrence. The first alternative is that the increase in ammonium with depth is possibly an abiotic result of upward ammonium transport from the landfill leachate plume. Furthermore, concentrations of ammonium will most likely continue to increase with increases in depth as the heart of the plume is approached. These results are analogous to the findings of Lorah et al., (2009). The second

alternative to explain the increase in ammonium with depth would be that this process is biotically charged and is a result of microbial cycling of iron and ammonium as mentioned above. Looking at iron (II) concentrations, NO_3^- concentrations, and ammonium concentrations collectively, it can be seen that iron (II) becomes depleted along with the NO_3^-, while the ammonium increases. This inverse relationship between the iron (II) and nitrate and ammonium suggests a microbially mediated redox process is at work. The last alternative is that the increase in ammonium with depth is a combination of both the abiotic and biotic processes explained above. This is the most likely alternative as indicators for both processes are present. As seen in Figure 14a and 14c, high concentrations of chloride and ammonium were present throughout the soil column, confirming that landfill leachate contaminates were present. Also, the decrease in iron (II) and subsequent increase in ammonium contributes to the strong possibility that a microbially mediated redox process was occurring. The degree to which each of the processes contributed to the concentrations of ammonium throughout the core, however, is not known.

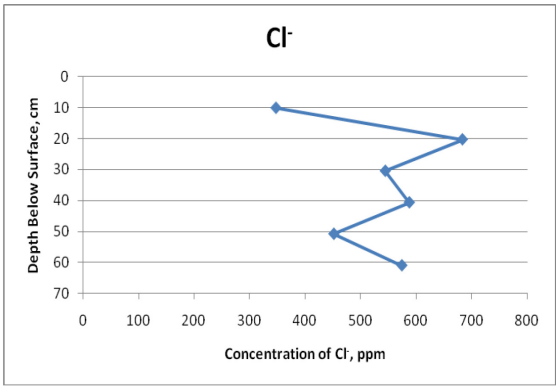

14a

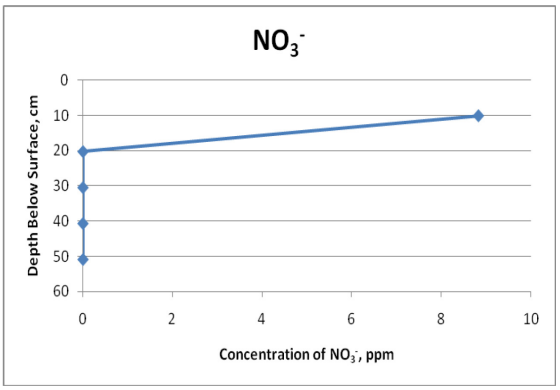

14b

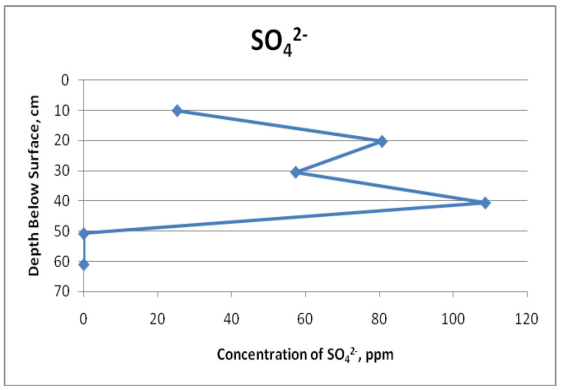

14c

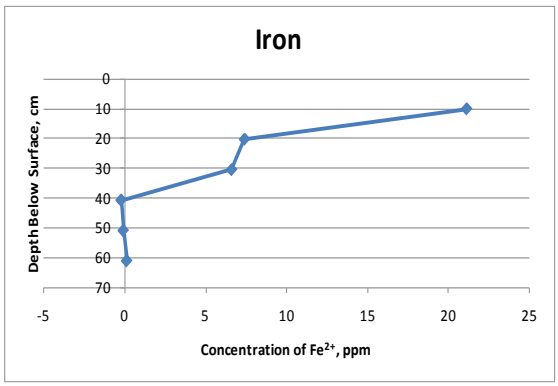

14d

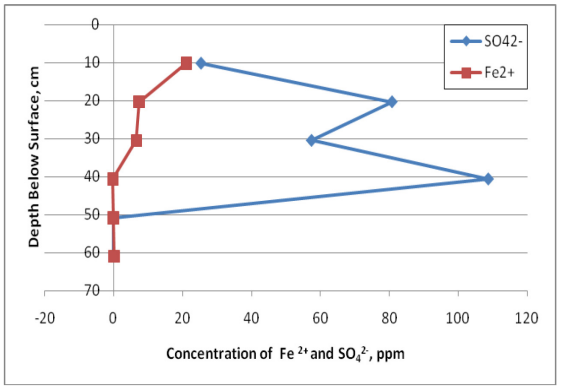

14e

Figure 14. Depth - concentration profiles for components of the anion geochemical parameter. 14a represents chloride concentrations with depth. 14b represents nitrate concentrations with depth. 14c represents sulfate concentrations with depth. 14d represents reduced iron concentrations with depth. 14e represents both reduced iron and sulfate concentrations with depth.

Anions, Iron (II), and Sulfate

Concentrations for chloride (Figure 14a) were significantly higher than any of the other anions, peaking at a maximum value of 683 ppm. These high concentrations of Cl^- within the core, which were in excess of 300 ppm, indicate the possible presence of leachate in the system from the nearby leachate plume. It is likely that the concentration of Cl^- will increase with depth and, similar to the concentration of ammonium, might peak at the center of the contaminate plume (Báez-Cazull et al., 2007). Recent studies have found that Cl^- can be used as a tracer to indicate the presence of leachate contaminated waters (Báez-Cazull et al., 2007; Grossman et al., 2002; Lorah et al., 2009; Roling et al., 2001; van Breukelen and Griffioen, 2004).

Figure 14c illustrates that nitrate is present in the uppermost section of the core with a concentration of 9 ppm. However, the concentration of nitrate decreases to zero in the remaining sections of the core. Nitrate, according to thermodynamics, should be one of the first alternate electron acceptors to be utilized by anaerobic bacteria in anoxic aquifers, leaving ammonium as the primary nitrogen species in the system. Ammonium originates from both active microbial cycling of wetland organic matter and transport from the landfill leachate plume (Báez-Cazull et al., 2007; Cozzarelli et al., 2000). The source of the initial show of nitrate at the surface likely results from surface run off of agricultural fertilizers (Knox and Canter, 1996).

Table 8. H_2S detection Result (mV) measured for each section of the core. All results for H_2S were below the detection limit (bdl) (< 0.001 ppm).

H_2S Detction Results (mV)		
Section 1	-442.1	bdl
Section 2	-527.8	bdl
Section 3	-552.7	bdl
Section 4	-563.9	bdl
Section 5	-537.4	bdl
Section 6	-544	bdl

The change in concentrations of sulfate and iron (II) with depth are shown in Figures 14d and 14e, respectively. Studies by Báez-Cazull et al., (2007) and Koretsky et al., (2003) found similar sulfate and iron profiles in wetland environments. Sulfate, which is an indicator of oxidative processes, is relatively low in the first section of the core. However, iron (II) is at its highest concentration in the same section. Moving down the core, the sulfate concentrations begin to increase while the iron concentrations start decreasing with increasing depth. At the same time, Table 8 reveals that no sulfide was present throughout the core. These contrasting quantities may indicate the occurrence of a redox process whereby reduced iron (II) phases became oxidized into iron (III). Results of previous studies support this hypothesis (Baez-Cazull et al., 2008; Hyacinthe and Van Cappellen, 2004; Luther III et al., 1992). The highest concentration of sulfate, which occurred at a depth of 40 cm at a concentration of 108 ppm, possibly resulted from a recharge event in the sandy section (aquifer) of the core. Scholl et al., (2006) associated high concentrations of sulfate with recharge events in aquifer environments. A significant recharge event would bring an influx of more oxygenated,

anaerobic water into the system enhancing the ability of redox processes to occur. At this section of the core, there is also a complete lack of any iron (II), which further confirms that a significant recharge event occurred. The findings of the sequential extractions, i.e. a high percentage of moderately reducible iron (III) phases, coupled with the results from the geochemical analysis, i.e. undetectable amount of iron (II); support the earlier hypothesis that the sand layer contained more crystalline ferric iron.

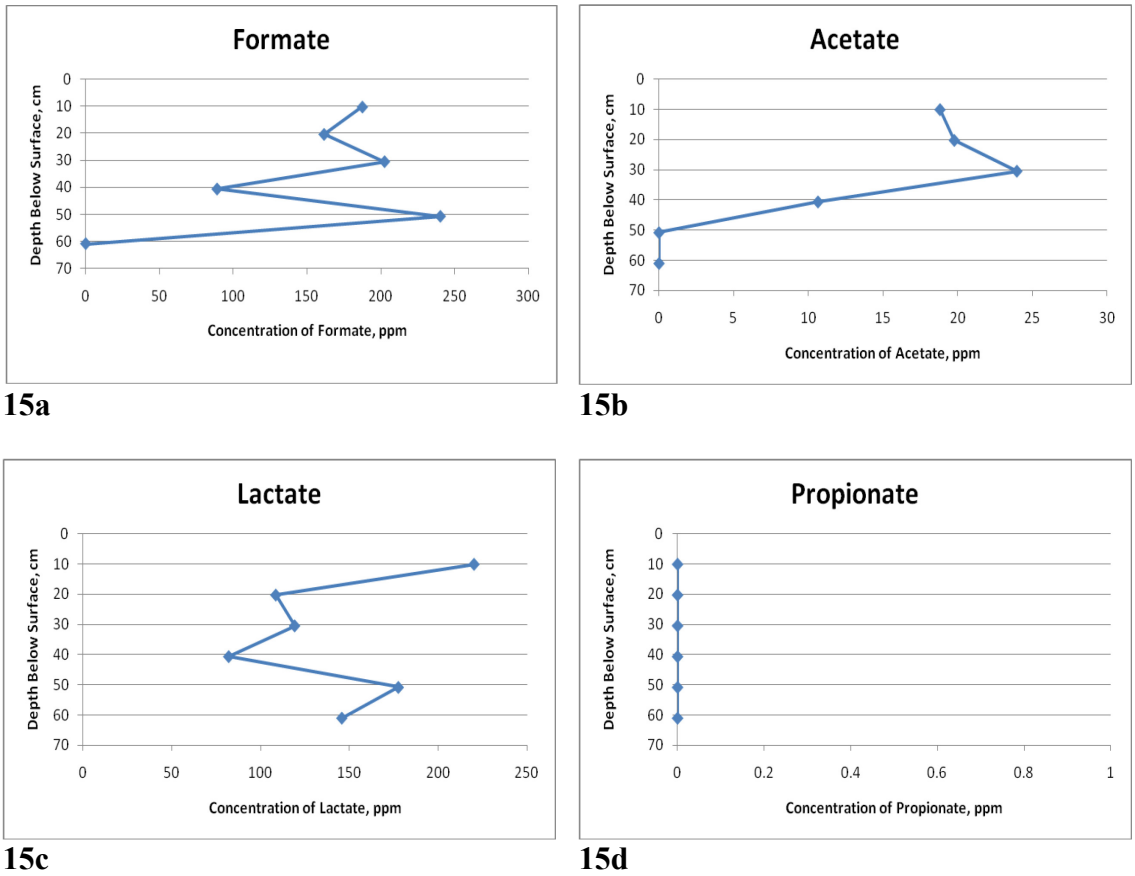

15a **15b**

15c **15d**

Figure 15. Depth - concentration profiles for components of the organic acid geochemical parameter. 15a represents the concentrations of formate with depth. 15b represents the concentrations of acetate with depth. 15c represents the concentrations of lactate with depth. 15d represents the concentrations of propionate with depth.

Organic Acids

Throughout the depth profiles, the organic acids generally decrease with depth, with the exception of propionate (Figure 15). The highest concentrations for each of the organic acids are 240 ppm at a depth of 50 cm, 24 ppm at a depth of 30 cm, and 220 ppm at a depth of 10 cm for formate, acetate, and lactate, respectively. Propionate was not detected at the depths studied in this research. The presence of the organic acids at the sediment-water interface is likely due to the degradation of the organic matter in the upper sediment layers of the slough. Due to the availability of electron acceptors at depth within slough sediments (Figure 15), the decreasing amount of organic acids may reflect microbial oxidative processes occurring; whereby organic acids are becoming depleted as they are oxidized into CO_2 by microbes (Chapelle 2001).

5.2 MICROBIAL COMMUNITIES' RESPONSE TO GEOCHEMICAL PERTURBATIONS VIA NOGEES

Two main findings are presented in this section: a microbial communities' response to geochemical perturbations, Figures 16 and 17 along with Table 9, and a DNA analysis to determine the amount of growth of geobacter due to geochemical perturbations, Figure 18. Figure 16 shows the concentration of iron (II) in the initial test solution (green line) and after exposure to the microbial communities in NOGEE I1 (blue line) and NOGEE I2 (red line). Figure 17 displays the rate at which the microbial communities in NOGEEs I1 and I2 can reduce iron (III). Figure 18 illustrates the

density of geobacter present in NOGEEs I1 and I2 as well as the density of geobacter present in the blank and dummy wells.

Table 9. Summary of exposure periods of ferrihydrite amended solution and iron (II) concentration results.

Run #	Iron NOGEEs	Time Exposed to Each Test Solution (hrs)	Cumulative Exposure Time to Amended Solutions	Concentration of Iron (II) (ppm)
	ITS I1			9.85
Run 1	I1-1	71.82	71.82	2.09
	I2-1	71.93	71.93	5.28
	ITS I2			9.46
Run 2	I1-2	47.52	119.33	7.32
	I2-2	47.57	119.50	8.22
	ITS I3			9.46
Run 3	I1-3	47.70	167.03	15.54
	I2-3	47.85	167.35	14.51
	ITS I4			7.88
Run 4	I1-4	47.45	214.48	14.98
	I2-4	47.47	214.82	18.80
	ITS I5			8.46
Run 5	I1-5	47.60	262.08	11.94
	I2-5	47.35	262.17	19.47

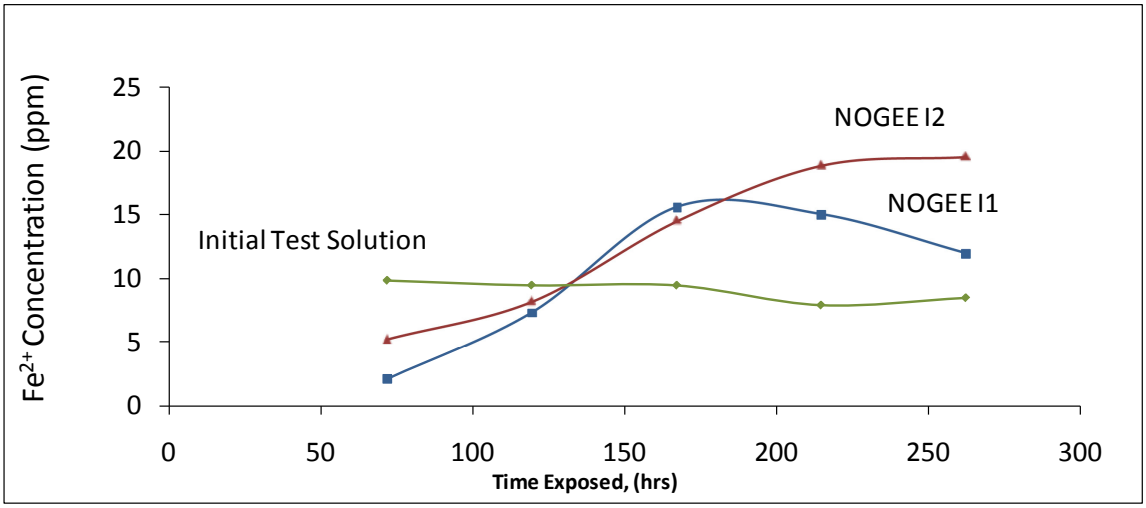

Figure 16. Iron (II) concentration with time for NOGEE's I1 and I2.

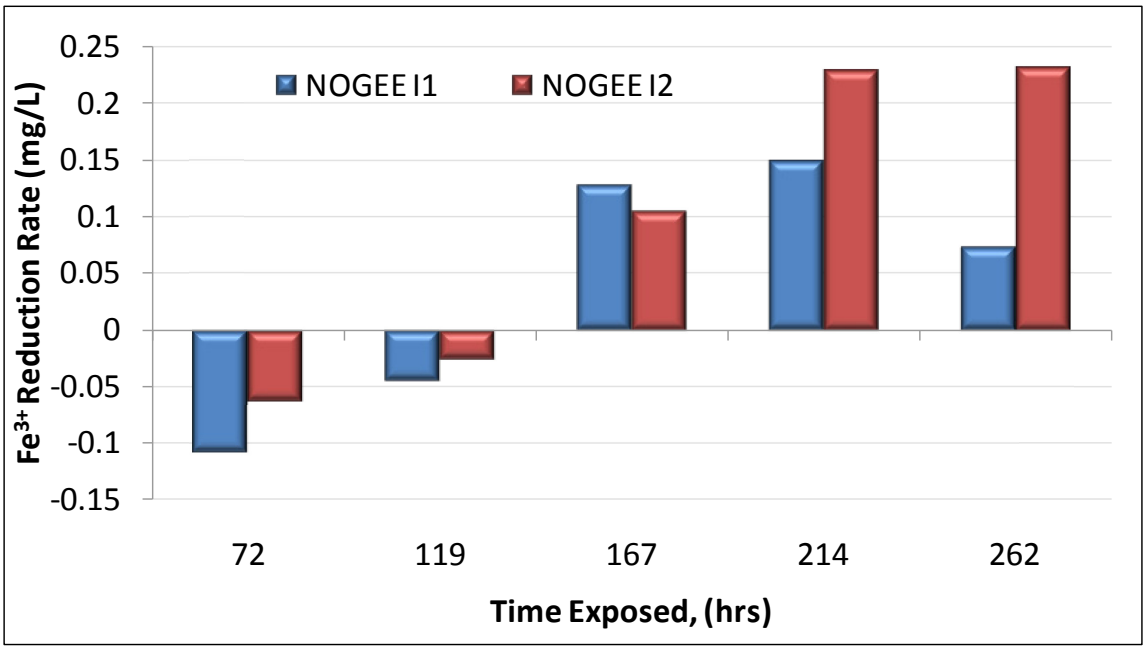

Figure 17. Iron (III) reduction rate over time.

The results of the experiments performed with the NOGEEs are presented in Figures 16 and 17, and Table 9 show that over the 11 day period the NOGEEs were subjected to the geochemically perturbed solution the microbial communities were able to effectively reduce ferrihydrite into an iron (II) phase. Although, laboratory microcosm studies have proven that microbially mediated iron reduction occurs in wetland sediments (Albrechtsen and Christensen, 1994; Lovley, 1991; Pulgarin and Kiwi, 1995; Roden and Wetzel, 2002; Thamdrup et al., 1993), this is the first time that iron (III) reduction has been observed in *in situ* environments. Due to inclement weather conditions, the first two data sampling periods could not be completed as intended. However, previous studies (Chapelle, 2001; McGuire et al., 2002) and extrapolation of the data suggest that a lag phase occurred as the microbes adjusted to the introduction of

the amended solution. Following the lag phase, both NOGEE I1 and I2 entered exponential growth phase between the first and third data points, as seen in Figure 16. Between the third and fourth addition of the perturbed solution, i.e. between data points 3 and 4, NOGEE I1 (blue line) began to decrease in iron (II) concentration. This occurs at an exposed time of 167 hrs (Table 9) and could indicate that the microbial communities inhabiting this NOGEE reached the death phase for that colony. There are several theories as to why this decrease in iron (II) production occurred in similar experiments. A study by Koretsky et al., (2003) found that iron reducing bacteria ceased to continue growth in the presence of sulfide reducing bacteria; however, the lack of sulfide in the amended solution should have prevented this. Chapelle et al., (1996) and Portier and Palmer (1989) theorized that an increase in the bioaccumulation of toxic microbial waste could result in the cessation of growth in a microbial community; leading to a death phase and concomitant decrease in iron (II) production. The microbial communities in NOGEE I2 appear to have reached the stationary phase following data point 4, as shown in Figure 16. The slowdown in the production of iron (II) could be a result of the bioaccumulation of toxic microbial waste preventing further growth of the microbial colony; however this was not sufficiently high during the sampling time to begin seeing a decline in the population.

As seen in Figures 16 and 17, there was an initial decrease in the concentration of iron (II) during the lag phase of the iron reducing bacteria. Emerson and Moyer (1997) discovered several strains of bacteria that are capable of oxidizing iron (II) to iron (III). A higher initial population of the iron oxidizing bacteria compared to the iron reducing

bacteria would explain the low early iron (II) concentration. The low concentrations of iron (II) in the amended test solution compared to the high concentrations of iron (III) could possibly lead to a decline in the population of the iron oxidizing bacteria and an increase in the population of the iron reducing bacteria, seen in Figures 16 and 17.

The polycarbonate, chemically-inert sponge that served as a colonization substrate within the NOGEE samplers was removed from the inner chamber of the NOGEE immediately after the wells were extracted from the wetland. Sponges were immediately preserved on dry ice for molecular assays of microbial community structure. These sediments were analyzed by Mary Voytek (USGS) and her team in Reston, Virginia for the quantity of geobacter per nanogram DNA. Geobacter was specifically targeted because it is a known iron-reducing microbial group. The results of this test revealed that microbial communities had colonized on each of the sponges in the blank NOGEEs (t_o) and their communities existed at varying magnitudes (Figure 18). Some of the blank NOGEEs showed that a smaller population existed within the microcosm when compared to the other blank NOGEEs. These differences between blank wells are likely a result of small scale heterogeneities in the wetland. Similar microbially heterogeneous distributions in aquifer environments have been found in other studies (Baez-Cazull, 2007; Báez-Cazull et al., 2007; Baez-Cazull et al., 2008; He et al., 2002; Kneeshaw, 2008). A comparison of the initial amount of geobacter/nanogram DNA in the blank NOGEEs (t_o) to the final amount in NOGEEs I1 and I2 shows that the iron reducing community specific to geobacter became more dominant following an 11 day period of subjection to a geochemically amended solution

(Figure 18). When introduced to a porewater solution amended with ferrihydrite, the microbial communities positively responded by expanding their population by a significant amount (mean abundance ~1.28E+04 +/- 535.29 copies geo/ng DNA). This was nearly half an order of magnitude when compared to the most populous blank NOGEE, and over an order of magnitude when compared to the least populated blank NOGEE (mean abundance 4.70E+03 copies geo/ng DNA). The wells that were amended with sulfate (NOGEEs S1 and S2) were not subjected to the amended solution of ferrihydrite. However, their microcosms were still populated with a community of geobacter (4.36E+03 copies geo/ng DNA) and showed a similar population to that of the blank NOGEEs. These results support the hypothesis that the microbial communities of geobacter will favorably respond to ferrihydrite as an electron donor, thus engaging in redox reactions, which ultimately contribute to bioremediation.

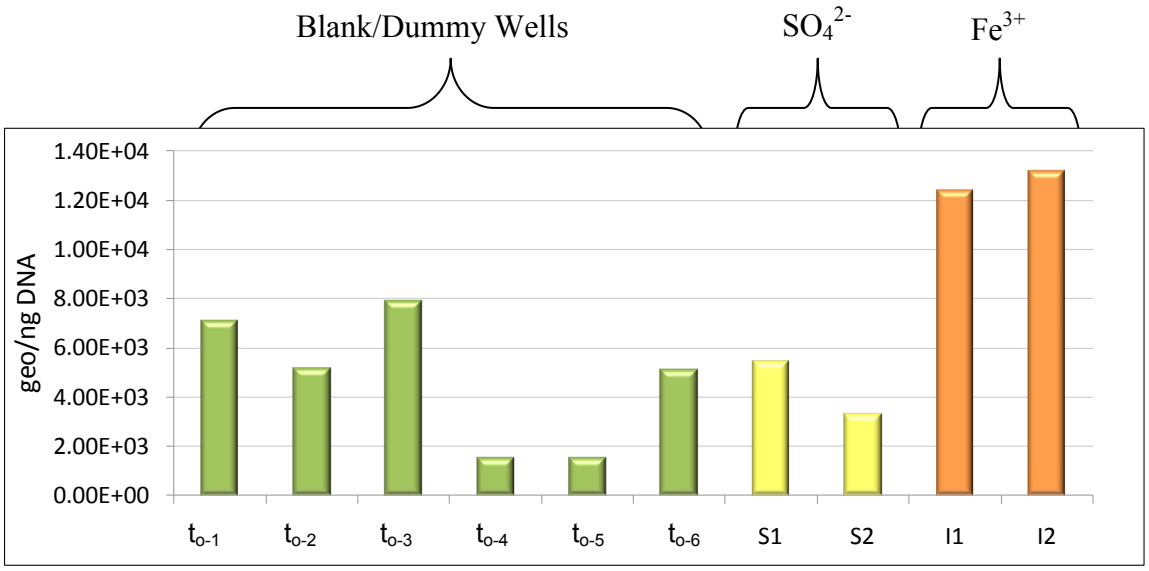

Figure 18. Amount of geobacter/nanogram (geo/ng) DNA present in each NOGEE. To bars represent results of sponges removed from each blank well. S1, S2, I1 and I2 show results of corresponding NOGEE's after 11 days of subjection to a geochemically perturbed solution amended with ferrihydrite. These data were run by Mary Voytek and her lab group at the USGS in Reston, Virginia.

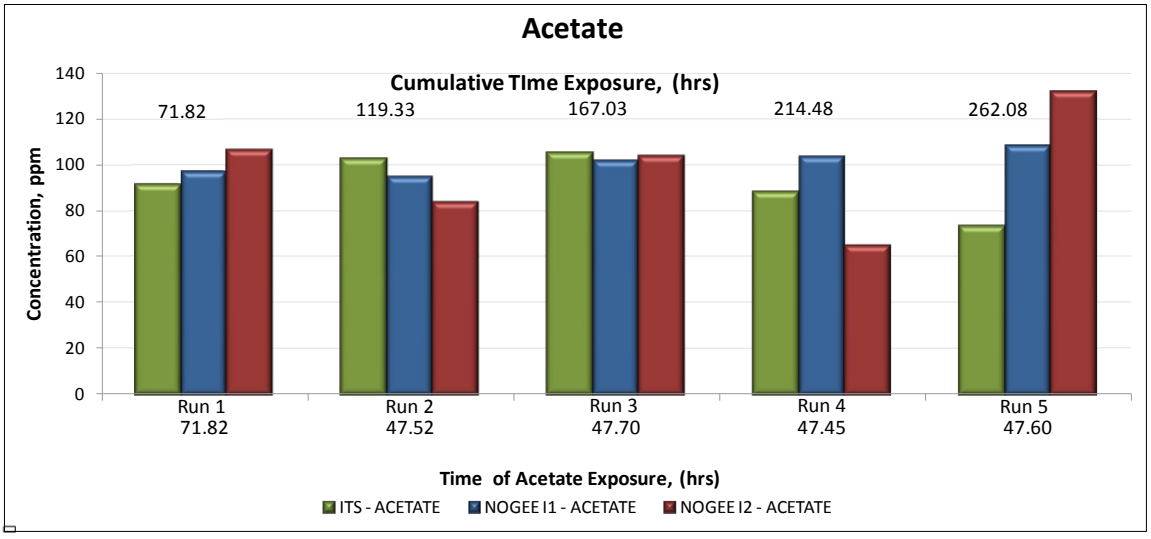

Figure 19. Acetate concentrations throughout NOGEE experimental procedure.

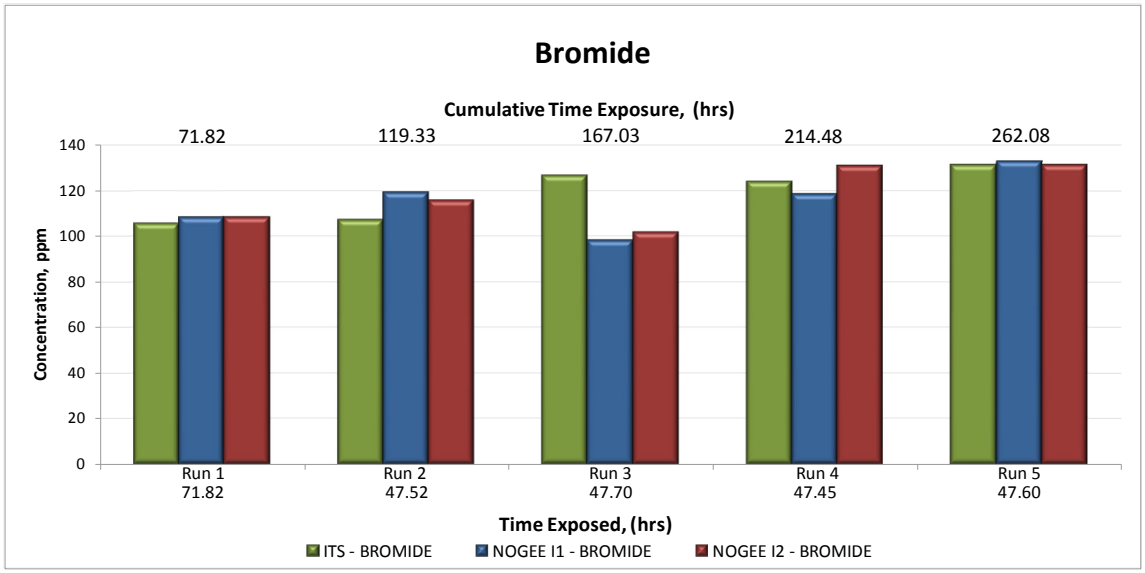

Figure 20. Bromide concentrations throughout NOGEE experimental procedure.

Figures 19 and 20 display how microbial communities respond to the introduction of acetate and bromide, respectively. Since the ITS geochemical samples were taken prior to being introduced into the well, any variability in either acetate or bromide concentrations were most likely due to random error by the researchers at the time of preparation. The acetate concentrations for the given incubation period for NOGEEs I1 and I2, shown in Figure 19, fluctuate throughout the experimental period. Despite these fluctuations, there was sufficient acetate for the microbial communities to remain active. NOGEE I2 during Run 4 culminated with the lowest concentration of acetate. However, it also produced the second highest Fe III reduction rate, shown in Figure 17, concluding sufficient acetate was remaining to fuel a continued, microbially-driven redox reaction. He et al., (2002) found that acetate played an essential role as a donor in redox processes. This is reasonable since the targeted microbial growth was

aimed toward iron reducing microbial communities which would oxidize acetate in association with the reduction of the ferrihydrite (Tor et al., 2001).

Bromide was added to the solution to act as a conservative tracer. Figure 20 shows that bromide increased about 25% throughout the experimental process. This overall increase is probably a result of an incomplete removal of the amended solution after each 48-hr subjection period. If residual test solution remained in the chamber of the NOGEEs after the test solution was removed, it would result in a slow, constant increase of bromide with each successive addition of amended test solution. Over all, the bromide acted as a sufficient tracer to indicate that the amended solutions were being almost completely removed after each subjection period.

The remainder of the geochemical parameters that were tested showed no significant changes throughout the experiment. However, these data were recorded and can be found in Appendix B.

5.3 AVS AND TRS EXTRACTIONS PREFORMED ON NOGEE SPONGES

AVS and TRS extraction procedures were performed on the sponges removed from each of the NOGEEs. The findings from these extractions show that AVS was only recovered in the first and second blank wells (Figure 21). TRS was evolved in several more of the NOGEEs. TRS appeared in four of the six blank wells, all but one of the iron NOGEEs, and in all three of the sulfate NOGEEs (Figure 22). However, control NOGEEs showed no TRS present. Similar heterogeneous distributions in aquifer environments have been found in other studies (Baez-Cazull, 2007; Báez-Cazull

et al., 2007; Baez-Cazull et al., 2008; He et al., 2002; Kneeshaw, 2008). Like the AVS and TRS results from the sequential extractions, these results are also questionable because of the late discovery of the need to titrate samples with HCl. It is possible that not performing this step may have led to a loss in data as well as inaccurate data results.

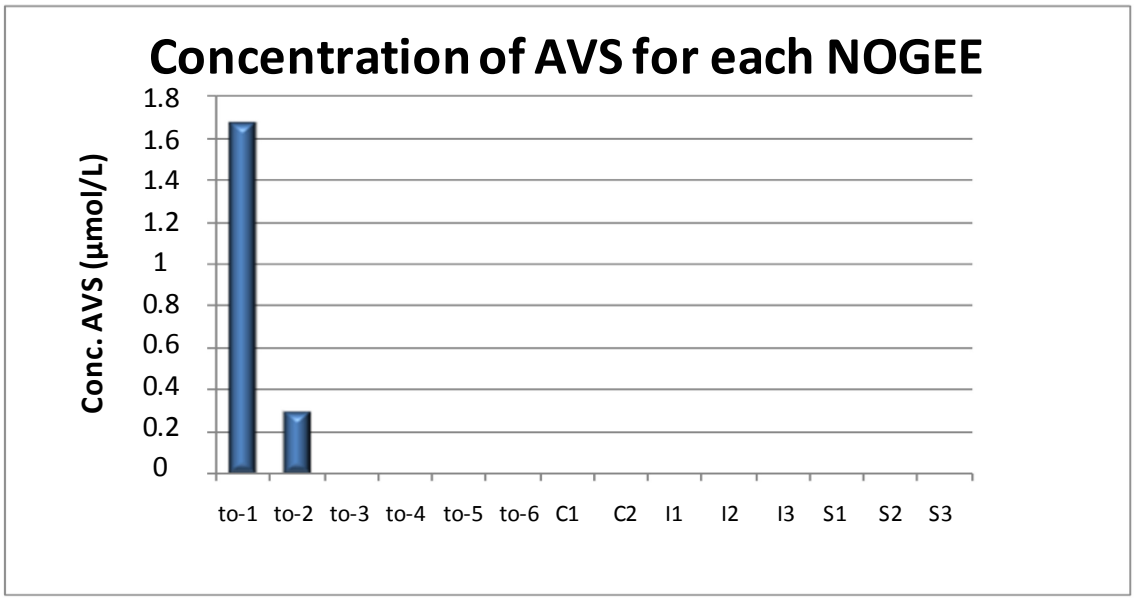

Figure 21. Concentration (µmol/L) of AVS present in each NOGEE.

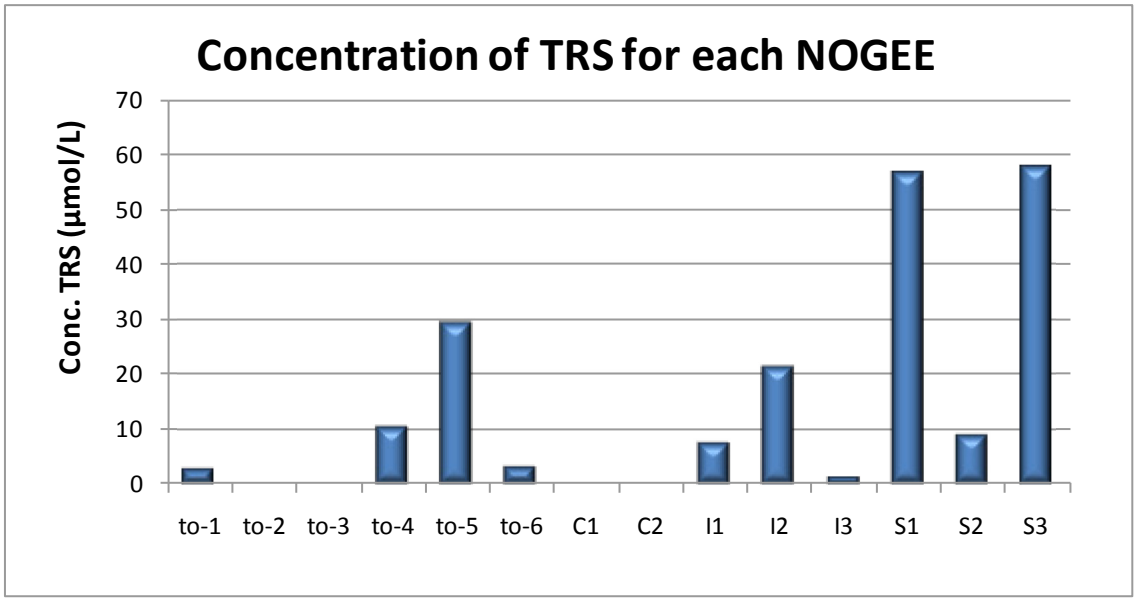

Figure 22. Concentration (µmol/L) of TRS present in each NOGEE.

6. CONCLUSIONS

The purpose of this research served to gain a better understanding of the temporal, spatial, and microbial controls on iron (III) in and around the Norman Oklahoma Landfill. The results of the first part of this study allowed us to understand qualitatively, as well as quantitatively, where different iron (III) phases reside with depth in the wetland-aquifer system. It was found that the most abundant iron (III) phases throughout the core were the weakly acid soluble iron phases. The shallow aquifer or sandy layers of Sections 4 and 5 presented the lowest amount of iron (III) phases overall While these layers had the lowest total concentrations of iron (III) phases, the phases that were the most abundant within these two sections were the moderately reducible phases, which is probably due to the constant influx of fresh water recharge.

The NOGEEs were used to discover if microbial communities would respond positively to an introduction of geochemically perturbed solutions. The findings from these experiments showed that the microbial communities not only responded to the solutions by reducing ferrihydrite to an iron (II) phase, but also increased their community population by a significant amount. The change in reduction of iron (III) for NOGEE I1 was a total of 13.45 ppm, increasing from an iron (II) concentration of 2.09 ppm to 15.54 ppm. NOGEE I2 had a total change in reduction of 14.19 ppm. The initial concentration of iron (II) for NOGEE I2 was 5.28 ppm and increased to a final concentration of 19.47. Geobacter, the iron reducing bacteria specifically analyzed in

this experiment, were found to have increased in population over the eleven day period by a mean of 1.28 E+04 +/-535.29 copies geo/ng DNA.

While this experiment was able to test for the overall change in population of the microbial communities, it was unable to account for changes in population as amended solution was removed and added to the NOGEEs. The removal or addition of amended solution may have resulted in possible loss of microbes from the polycarbonate sponge. This may have introduced a slight decrease in the amount of reduction of iron (III) throughout the experiment. Ultimately, this experiment was able to prove that geobacter positively responded to the addition of amended solution through increased iron (III) reduction over an extended time period and successfully increased in population. However, taking in account the microbial growth rates at each addition of amended solution is something that should be considered in future studies.

This study is the first attempt to perform *in situ* tests on microbial communities in the slough. This methodology can now be expanded to other study sites and utilized by researchers to test microbial communities for their ability to biodegrade contaminates and the rates at which they perform these processes.

These results give us some insight into the iron cycling and controls that occur within this system. However, to gain an even better understanding of this system it would be prudent to perform more studies using different variables including, but not limited to:

- Differences between seasonal temperature changes
- Effects of weather on the system

- Amended NOGEEs with other iron oxide phases to explore if the microbial communities will respond more favorably to one phase over another
- Quantification of the population and type of each microbial community for the NOGEE experiments

REFERENCES

Ahnstrom, Z. S., Parker, D. R., 1999. Development and assessment of a sequential extraction procedure for the fractionation of soil cadmium. *Soil Science Society of America* **63**, 1650-1658.

Albrechtsen, H. J., Christensen, T. H., 1994. Evidence for microbial iron reduction in a landfill leachate-polluted aquifer. *Applied and Environmental Microbiology* **60**, 3920-3925.

Baez-Cazull, S., 2007. Spatial and temporal controls on biogeochemical indicators at the small-scale interface between a contaminated aquifer and wetland surface water, Dept. of Geology and Geophysics, Texas A&M University, PhD Dissertation.

Báez-Cazull, S., McGuire, J., Cozzarelli, I., Raymond, A., Welsh, L., 2007. Centimeter-scale characterization of biogeochemical gradients at a wetland-aquifer interface using capillary electrophoresis. *Applied Geochemistry* **22**, 2664-2683.

Baez-Cazull, S., McGuire, J., Cozzarelli, I., Voytek, M., 2008. Determination of dominant biogeochemical processes in a contaminated aquifer-wetland system using multivariate statistical analysis. *Journal of Environmental Quality* **37**, 30-46.

Baun, A., Reitzel, L. A., Ledin, A., Christensen, T. H., and Bjerg, P. L., 2003. Natural attenuation of xenobiotic organic compounds in a landfill leachate plume. *Contaminant Hydrology* **65,** 269-291**.**

Bonneville, S., Van Cappellen, P., Behrends, T., 2004. Microbial reduction of iron(III) oxyhydroxides: effects of mineral solubility and availability. *Chemical Geology* **212**, 255-268.

Canfield, D. E., Raiswell, R., Westrich, J. T., Reaves, C. M., Berner, R. A., 1986. The use of chromium reduction in the analysis of reduced inorganic sulfur in sediments and shales. *Chemical Geology* **54**, 149-155.

Chapelle, F., 2001. *Ground-water microbiology and geochemistry*; 2nd Edition, John Wiley & Sons Inc., New York, New York.

Chapelle, F. H., Haack, S. K., Adriaens, P., Henery, M. A., Bradley, P. M., 1996. Comparison of Eh and H2 measurements for delineating redox processes in a contaminated aquifer. *Environmental Science Technology* **30**, 3565-3569.

Christensen, T. H., Bjerg, P. L., Banwart, S. A., Jakobsen, R., Heron, G., Albrechtsen, H., 2000. Characterization of redox conditions in groundwater contaminat plumes. *Journal of Contaminant Hydrology* **45**, 165-241.

Christenson, S., Cozzarelli, I. M., 1999. Geochemical and microbiological processes in groundwater and surface water affected by municipal landfill leachate*., Proceedings of the Technical Meeting, U. S. Geological Survey Toxic Substances Hydrology Program,* Charleston SC March 8-12 **3**, 499-500.

Christenson, S., Scholl, M. A., Schlottmann, J. L., and Becker, C. J., 1999. Ground-water and surface-water hydrology of the norman landfill research site*., Proceedings of the Technical Meeting, U. S. Geological Survey Toxic Substances Hydrology Program,* Charleston SC March 8-12 **3**, 501.

Clement, J., Shrestha, J., Ehrenfeld, J. G., Jaffe, P. R., 2005. Ammonium oxidation coupled to dissimilatory reduction of iron under anaerobic conditions in wetland soils. *Soil Biology & Biochemistry* **37**, 2323-2328.

Cornell, R. M., Schwertmann, U., 2003. *The iron oxides: structure, properties, reactions, occurrences and uses*. 2nd Edition, John Wiley & Sons Ltd, Weinheim, Germany.

Cornwell, J., Morse, J., 1987. The characterization of iron sulfide minerals in anoxic marine sediments. *Mar. Chem* **22**, 193-206.

Cozzarelli, I. M., Suflita, J. M., Ulrich, G. A., Harris, S. H., Scholl, M. A., Schlottmann, J. L., Christenson, S., 2000. Geochemical and microbiological methods for evaluating anaerobic processes in an aquifer contaminated by landfill leachate. *Environmental Science Technology* **34**, 4025-4033.

Crapse, K. P., Serkiz, S. M., Pishko, A. L., Barr, C. S., Brewer, K., Lee, C. M., and Schank, A., 2005. From sequential extraction to transport modeling, monitored natural attenuation as a remediation approach for inorganic contaminants. In: Clark, C. J., Stephenson Lindner, A., *Remediation of Hazardou Waste in the Subsurfac*. American Chemical Society, University of Florida, pp. 11-23.

Emerson, D., Moyer, C., 1997. Isolation and characterization of novel iron-oxidizing bacteria that grow at circumneutral pH. *Applied and Environmental Microbiology* **63**, 4784-4792.

Grossman, E., Cifuentes, L., Cozzarelli, I., 2002. Anaerobic methane oxidation in a landfill-leachate plume. *Environ. Sci. Technol* **36**, 2436-2442.

He, J., Sung, Y., Dollhopf, M., Fathepure, B., Tiedje, J., and Lˆffler, F., 2002. Acetate versus hydrogen as direct electron donors to stimulate the microbial reductive dechlorination process at chloroethene-contaminated sitesÜ. *Environ. Sci. Technol* **36**, 3945-3952.

Heron, G., Crouzet, C., Bourg, A. C. M., and Christensen, T. H., 1994. Speciation of Fe(II) and Fe(III) in contaminated aquifer sediments using chemical extraction techniques. *Environmental Science Technology* **28**, 1698-1705.

Hyacinthe, C., Bonneville, S., Van Cappellen, P., 2006. Reactive iron(III) in sediments: chemical versus microbial extractions. *Geochimica et Cosmochimica Acta* **70**, 4166-4180.

Hyacinthe, C., Van Cappellen, P., 2004. An authigenic iron phosphate phase in estuaring sediments: composition, formation, and chemical reactivity. *Marine Chemistry* **91**, 227-251.

Kneeshaw, T., 2008. Evaluation of kinetic controls on sulfate reduction in a contaminated wetland-aquifer system, Dept. of Geology and Geophysics, Texas A&M University, PhD Dissertation.

Knox, R., Canter, L., 1996. Prioritization of ground water contaminants and sources. *Water, Air, & Soil Pollution* **88**, 205-226.

Kolthoff, I. M., Elving, P. J., 1993. *Treatise on analytical chemistry*. 2nd Edition, Wiley, John & Sons, New York.

Koretsky, C. M., Moore, C. M., Lowe, K. L., Meile, C., DiChristina, T. J., and Van Cappellen, P., 2003. Seasonal oscillation of microbial iron and sulfate reduction in saltmarsh sediments. Springer, Sapelo Island, GA,

Larsen, O., Postma, D., 2001. Kinetics of reductive bulk dissolution of lepidocrocite, ferrihydrite, and goethite. *Geochemica at Cosmochimica Acta* **65**, 1367-1379.

Li, L., Pan, Y., Wu, Q., Zhou, X., Li, Z., 1988. Amorphous iron oxide as an electron acceptor for ammonium oxidation under anaerobic conditions. *Acta Pedol. Sin* **25**, 184-190.

Lorah, M., Cozzarelli, I., Bˆhlke, J., 2009. Biogeochemistry at a wetland sediment-alluvial aquifer interface in a landfill leachate plume. *Journal of Contaminant Hydrology* **105**, 99-117.

Lovley, D. R., 1997. Microbial Fe(III) reduction in subsurface environments. *FEMS Microbiology Reviews* **20**, 305-313.

Lovley, D. R., Phillips, E. J. P., 1986. Availability of ferric Fe for microbial reduction in bottom sediments of freshwater tidal Potomac River. *Applied and Environmental Microbiology* **52**, 751-757.

Lovley, D. R., 1991. Dissimilatory Fe (III) and Mn (IV) reduction. *Microbiological Reviews* **55,** 259-287.

Luther III, G., Kostka, J., Church, T., Sulzberger, B., Stumm, W., 1992. Seasonal iron cycling in the salt-marsh sedimentary environment: the importance of ligand complexes with Fe (II) and Fe (III) in the dissolution of Fe (III) minerals and pyrite, respectively. *Marine Chemistry* **40**, 81-103.

McGuire, J. T., Long, D. T., Klug, M. J., Haack, S. K., Hyndman, D. W., 2002. Evaluating behavior of oxygen, nitrate, and sulfate during recharge and quantifying reduction rates in a contaminated aquifer. *Environmental Science Technology* **36**, 2693-2700.

McGuire, J. T., Smith, E. W., Long, D. T., Hyndman, D. W., Haack, S. K., Klug, M. J., and Velbel, M. A., 2000. Temporal variations in parameteres refecting terminal-electron-accepting-processes in an aquifer contaminated with waste fuel and chlorinated solvents. *Chemical Geology* **169**, 471-485.

Peltier, E., Dahl, A. L., Gaillard, J.-F., 2005. Metal speciation in anoxic sediments: when sulfides can be construed as oxides. *Environmental Science Technology* **39**, 311-316.

Portier, R., Palmer, S., 1989. *Wetlands microbiology: form, function, processes*. Lewis Publishers, Chelsea, Michigan.

Poulton, S. W., Canfield, D. E., 2005. Development of a sequential extraction procedure for iron: implications for iron partitioning in continentally derived particulates. *Chemical Geology* **214**, 209-221.

Pulgarin, C., Kiwi, J., 1995. Iron oxide-mediated degradation, photodegradation, and biodegradation of aminophenols. *Langmuir* **11**, 519-526.

Raiswell, R., Canfield, D. E., Berner, R. A., 1993. A comparison of iron extraction methods for the determingation of degree of pyritisation and the recognition of iron limited pyrite formation. *Chemical Geology* **111**, 101-110.

Rapin, F., Tessier, A., Campbell, P. G. C., Carignan, R., 1986. Potential artifacts in the determination of metal partitioning in sediments by sequential extraction procedure. *Environmental Science Technology* **20**, 836 - 840

Raven, K. P., Jain, A., Loeppert, R. H., 1998. Arsenite and arsenate adsorption on ferrihydrite: kinetics, equilibrium, and adsorption envelopes. *Environmental Science Technology* **32**, 344-349.

Reese, B. K., Finneran, D. W., Morse, J. W., Zhu, M. X., 2009. Examination and refinement of the determination of aqueous hydrogen sulfide by the methylene blue method. *Environmental Science and Technology* (In Press).

Roden, E., Wetzel, R., 2002. Kinetics of microbial Fe (III) oxide reduction in freshwater wetland sediments. *Limnology and Oceanography*, **47**, 198-211.

Roden, E. E., Wetzel, R. G., 1996. Organic carbon oxidation and suppression of methane production by microbial Fe(III) oxide reduction in vegetated and unvegetated freshwater wetland sediments. *American Society of Liumology and Oceanography, Inc.* **41**, 1733-1748.

Roling, W., van Breukelen, B., Braster, M., Lin, B., van Verseveld, H., 2001. Relationships between microbial community structure and hydrochemistry in a landfill leachate-polluted aquifer. *Applied and Environmental Microbiology* **67**, 4619-4629.

Schlesinger, W. H., 1997. *Biogeochemisty: an analysis of global change*; 2nd Edition, Elsevier, San Diego, California.

Schlottmann, J. L., 2001. Water chemistry near the closed Norman landfill, Cleveland County, Oklahoma, 1995. *United States Geological Survey Water Resources Investigations Report 00-4238*, 44 p.

Scholl, M., Cozzarelli, I., Christenson, S., 2006. Recharge processes drive sulfate reduction in an alluvial aquifer contaminated with landfill leachate. *Journal of Contaminant Hydrology* **86**, 239-261.

Schwertmann, U., Cornell, R. M., 2000. *Iron Oxides in the Laboratory*. 2nd Edition, Wiley-VCH, Wienheim, Germany.

Scrow, K., Hicks, K. A., 2005. Natural attenuation and enchanced bioremediation of contaminants in groundwater. *Current Opinion in Biotechnology* **16**, 246--253.

Sorensen, J., 1982. Reduction of ferric iron in anaerobic, marine sediment and interaction with reduction of nitrate and sulfate. *Applied and Environmental Microbiology* **43**, 319-324.

Stookey, L. L., 1970. Ferrozine: a new spectrophotometric reagent for iron. *Analytical Chemistry* **42**, 770-781.

Tessier, A., Campbell, P. G. C., Bisson, M., 1979. Sequential extraction procedure for the speciation of particulate trace metals. *Analytical Chemistry* **51**, 844-851.

Thamdrup, B., 2000. Microbial manganese and iron reduction in aquatic sediments. *Advances in Microbial Ecology* **16**, 41-84.

Thamdrup, B., Finster, K., Hansen, J., Bak, F., 1993. Bacterial disproportionation of elemental sulfur coupled to chemical reduction of iron or manganese. *Applied and Environmental Microbiology* **59**, 101-108.

Tokalioglu, S., Kartal, S., Birol, G., 2003. Application of a three-stage sequential extraction procedure for the determination of extractable metal contents in highway soils. *Turk J Chem* **27**, 333-346.

Tor, J., Kashefi, K., Lovley, D., 2001. Acetate oxidation coupled to Fe (III) reduction in hyperthermophilic microorganisms. *Applied and Environmental Microbiology* **67**, 1363-1365.

Van Bodegom, P. M., Van Reeven, J., Denier Van Der Gon, A. C., 2003. Prediction of reducible soil iron content from iron extraction data. *Biogeochemistry* **64**, 231-245.

van Breukelen, B., Griffioen, J., 2004. Biogeochemical processes at the fringe of a landfill leachate pollution plume: potential for dissolved organic carbon, Fe (II), Mn (II), NH4, and CH4 oxidation. *Journal of Contaminant Hydrology* **73**, 181-205.

Vroblesky, D. A., Chapelle, F. H., 1994. Temporal and spatial changes of terminal electron-accepting processes in a petroleum hydrocarbon-contaminated aquifer and the significance for contaminant biodegradation. *Water Resources Research* **30**, 1561-1570.

Weber, K. A., Achenbach, L. A., Coates, J. D., 2006a. Microorganisms pumping iron: anaerobic microbial iron oxidation and reduction. *Nature Publishing Group* **4**, 752-764.

Weber, K. A., Urrutia, M. M., Churchill, P. F., Kukkadapu, R. K., Roden, E. E., 2006b. Anaerobic redox cycling of iron by freshwater sediment microorganisms. *Environmental Microbiology* **8**, 100-113.

Weiss, J. V., Emerson, D., Megonigal, J. P., 2004. Geochemical control of microbial Fe(III) reduction potential in wetlands: comparison of the rhizosphere to non-rhizosphere soil. *FEMS Microbiology Ecology* **48**, 89-100.

Welsh, L. W., 2007. Burial and decomposition of particulate organic matter in a temperate, siliciclastic, seasonal wetland. Dept. of Geology and Geophysics, Tx A&M University, M.S. Thesis.

Wilson, R. D., Thornton, S. F., Mackay, D. M., 2004. Challenges in monitoring the natural attenuation of spatially variable plumes. *Biodegradation* **15**, 359-369.

APPENDIX A

XRD ANALYSIS OF CORE SECTIONS

Table A. XRD peak values showing the first three highest intensities (I) for iron oxides. Lattice spacing was measured in Angstroms (dÅ).

Iron Oxide Mineral	esitmated 2θ	d(Å)	I	Iron Oxide Mineral	estimated 2θ	d(Å)	I
Hematite	32.80	2.700	100	**Ferrihydrite**	35.50	2.500	100
	34.60	2.591	70		40.60	2.210	80
	54.50	1.694	45		46.10	1.960	80
Maghemite	35.70	2.514	100	**Feroxyhyte**	35.12	2.560	100
	63.00	1.474	40		40.30	2.230	85
	30.20	2.950	30		54.00	1.700	65
Magnetite	35.40	2.532	100	**Schwetmanite**	35.11	2.550	100
	62.50	1.485	40		26.20	3.390	46
	56.80	1.616	30		35.11	2.550	37
Goethite	21.20	4.183	100	**Ankerite**	30.70	2.910	100
	36.80	2.450	50		50.40	1.801	45
	33.10	2.693	35		40.40	2.207	30
Lepidocrocite	27.00	3.294	100	**Siderite**	32.00	2.793	100
	36.30	2.473	76		24.40	3.592	30
	47.10	1.935	72		53.20	1.731	30
Akaganéite	11.90	7.400	100				
	28.50	3.311	100				
	35.30	2.543	80				

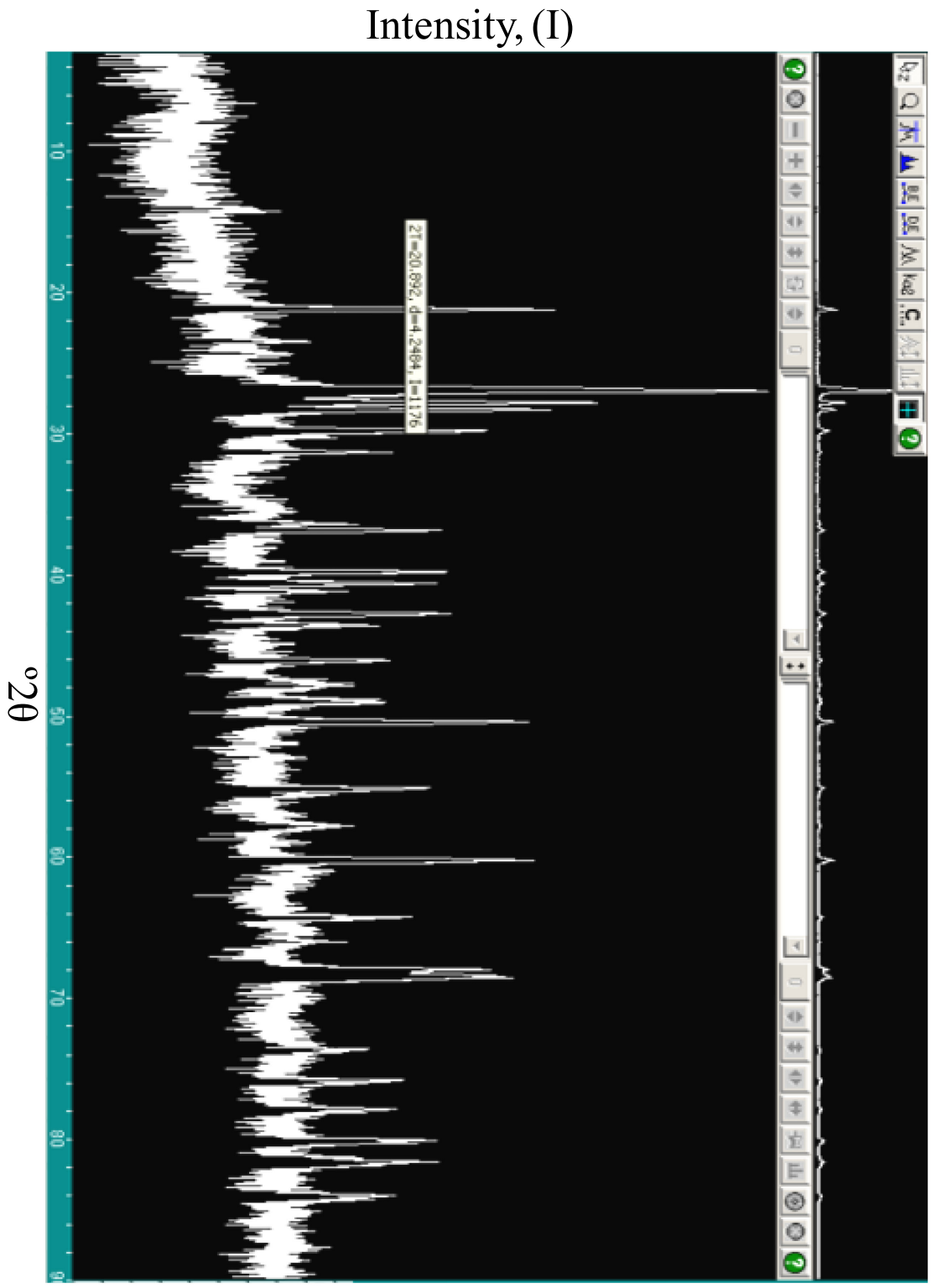

Figure A-1: Section 1 XRD analysis. X-axis scale is in º2θ,Y-axis scale is intensity (I).

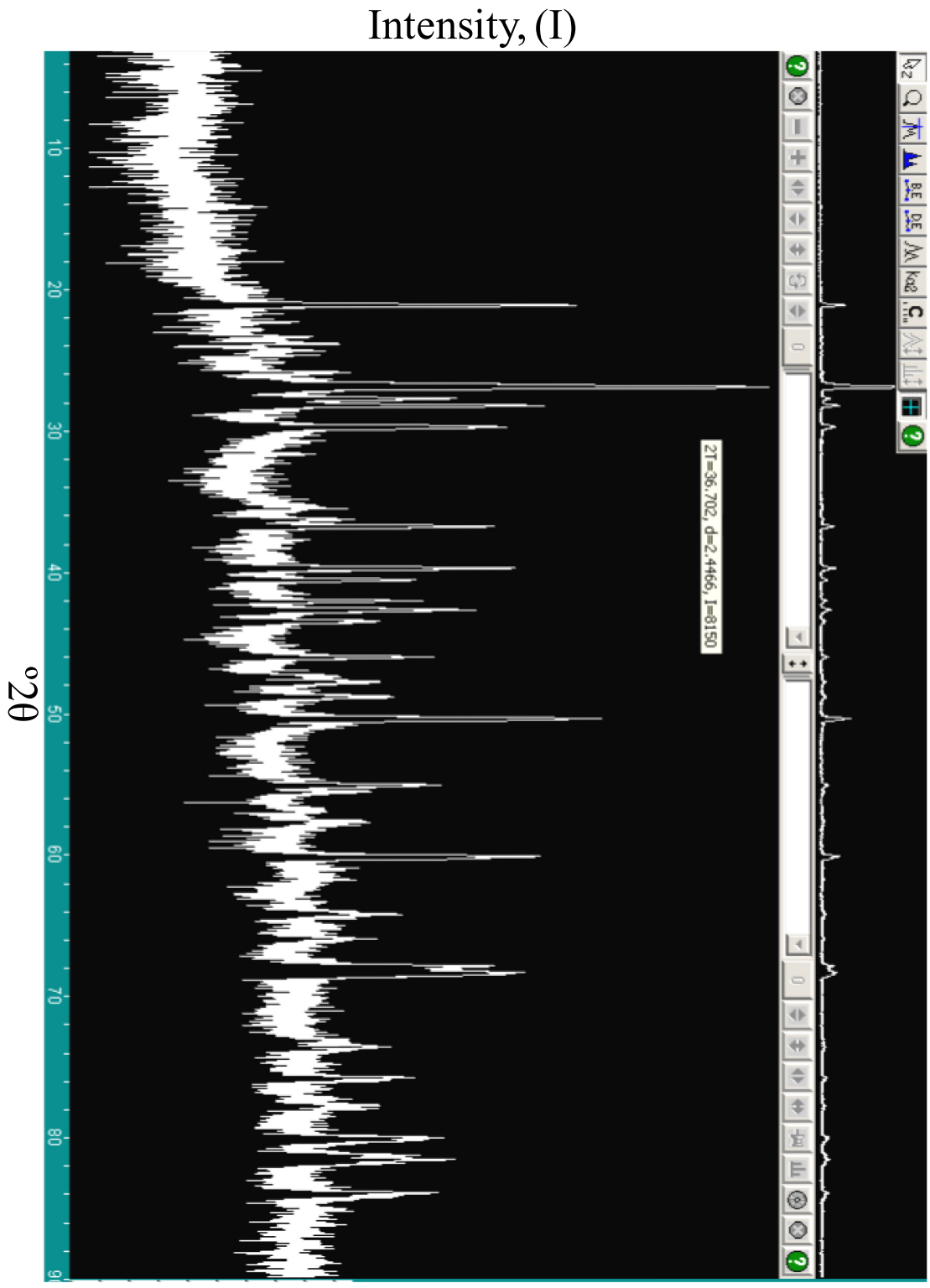

Figure A-2. Section 2 XRD analysis. X-axis scale is in º2θ, Y-axis scale is intensity (I).

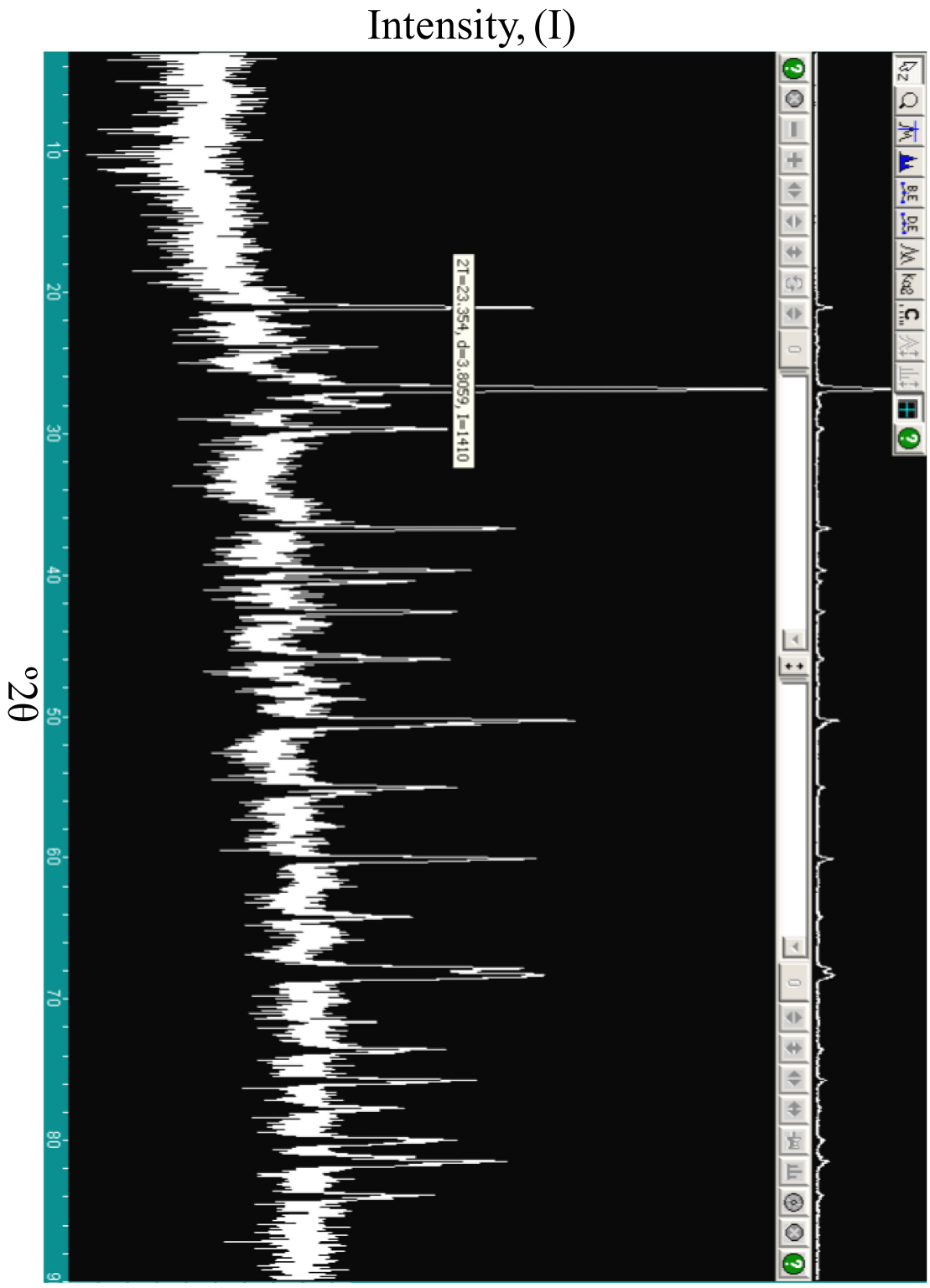

Figure A-3. Section 3 XRD analysis. X-axis scale is in º2θ, Y-axis scale is intensity (I).

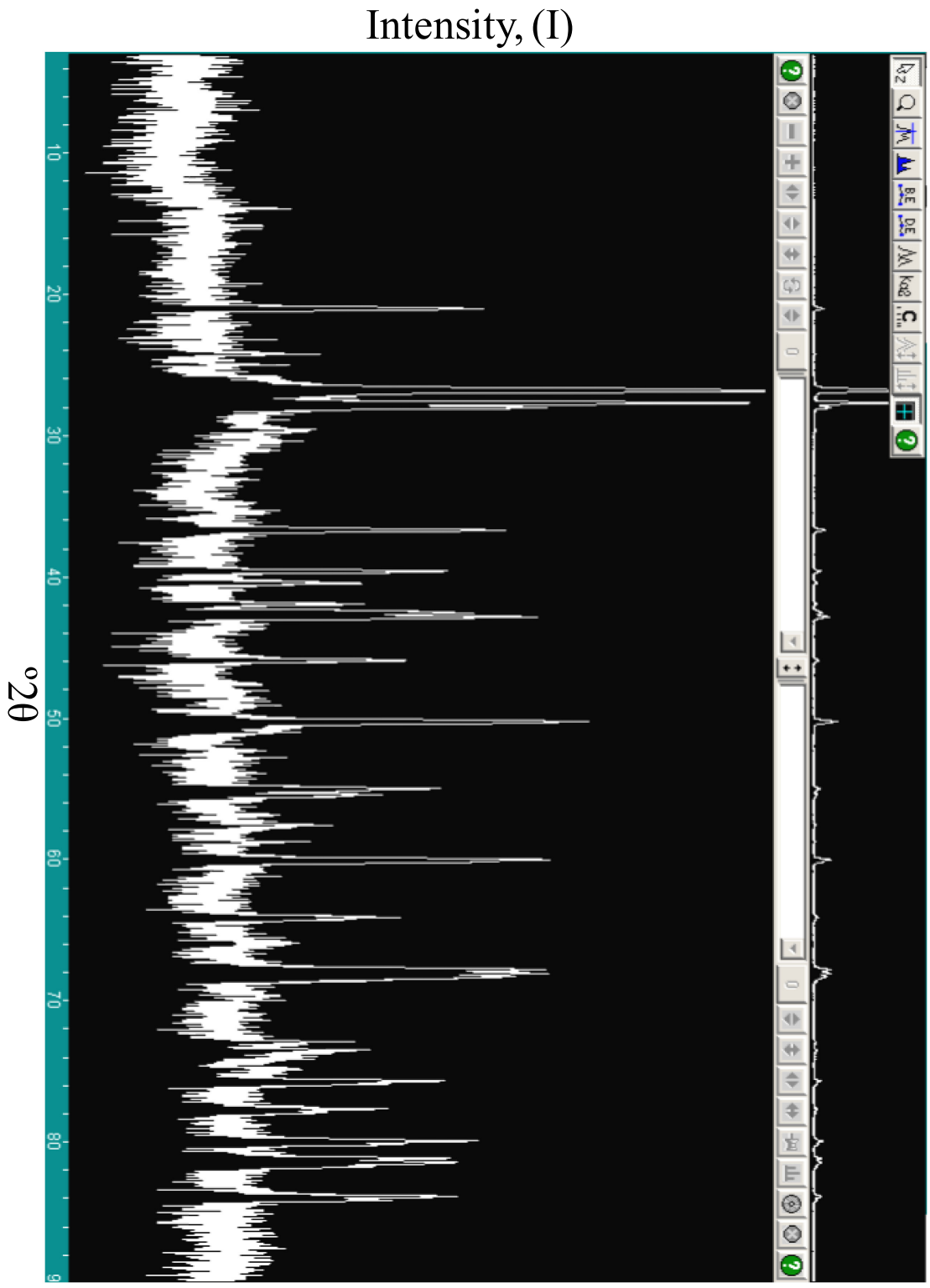

Figure A-4. Section 4 XRD analysis. X-axis scale is in º2θ, Y-axis scale is intensity (I).

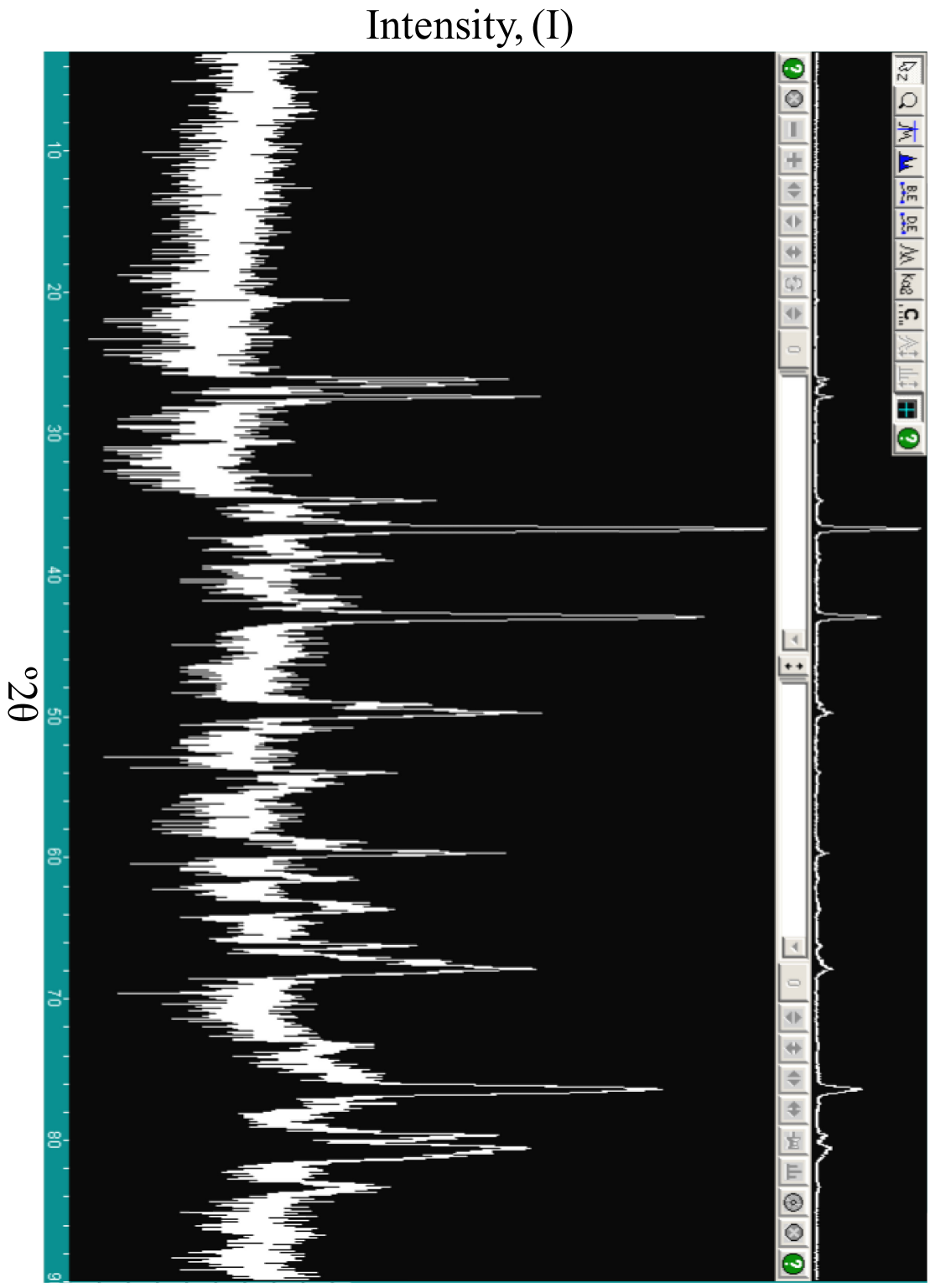

Figure A-5. Section 5 XRD analysis. X-axis scale is in º2θ, Y-axis scale is intensity (I).

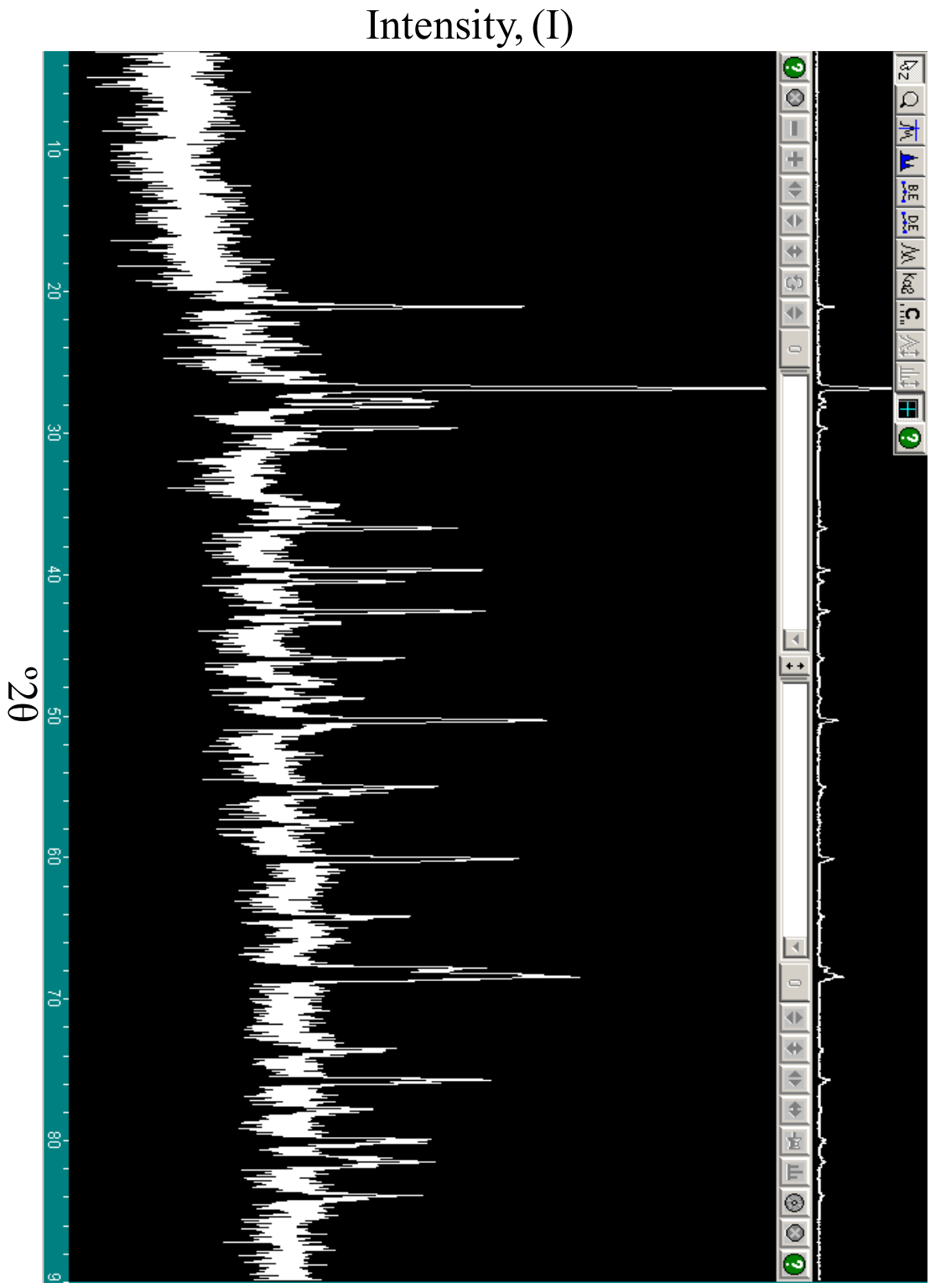

Figure A-6: Section 6 XRD analysis. X-axis scale is in º2θ, Y-axis scale is intensity (I).

APPENDIX B

RESULTS OF GEOCHEMICAL AND MOLECULAR ANALYSIS PERFORMED FOR NOGEE EXPERIMENT

Table B-1. Summary of geochemical parameters collected for NOGEE experiment.

Run #	Iron NOGEEs	Time Exposed to Test Solution (hrs)	Total Exposed Time (hrs)	CHLORIDE (ppm)	BROMIDE (ppm)	SULFATE (ppm)	NITRATE (ppm)	ACETATE (ppm)	AMMONIUM (ppm)	SULFIDE (ppm)	IRON (ppm)	Alkalinty (mmol/L)	Methane (ppm)	DOC (ppm of C)
	t_{o-1}			516.4	< 0.01	279.5	< 0.06	< 0.01	13.07	0.78	< 0.01	0.00	0.17	54.0
	t_{o-2}			558.2	< 0.01	331.7	< 0.06	< 0.01	0.53	0.07	< 0.01	0.00	0.12	59.5
	t_{o-3}			502.3	8.9	36.3	5.1	< 0.01	4.90	1.13	< 0.01	0.00	0.28	67.8
	t_{o-4}			524.4	5.7	266.5	1.8	< 0.01	0.48	0.31	< 0.01	0.00	0.20	54.2
	t_{o-5}			509.0	6.3	90.8	< 0.06	< 0.01	2.54	0.10	< 0.01	0.00	0.35	56.6
	t_{o-6}			489.5	5.6	45.1	< 0.06	< 0.01	< 0.01	1.11	< 0.01	0.00	0.22	55.3
	I1 initial			363.9	< 0.01	191.4	< 0.06	< 0.01	47.97	0.10	< 0.01	0.00	0.96	95.7
	I2 initial			391.0	13.5	121.6	< 0.06	< 0.01	18.78	1.22	< 0.01	0.00	1.96	111.1
	ITS I1			683.2	105.3	< 0.01	< 0.06	90.85	63.22	< 0.001	9.85	0.00	2.29	187.5
Run 1	I1-1	71.82	71.82	661.9	108.0	< 0.01	< 0.06	96.28	143.08	< 0.001	2.09	48.57	no sample	ND
	I2-1	71.93	71.93	714.2	108.0	< 0.01	< 0.06	105.91	179.85	< 0.001	5.28	59.16	1.81	182.6
	ITS I2			706.4	106.7	< 0.01	< 0.06	102.07	no sample	< 0.001	9.46	52.07	3.33	146.5
Run 2	I1-2	47.52	119.33	737.0	118.9	< 0.01	< 0.06	93.97	no sample	< 0.001	7.32	56.39	no sample	196.4
	I2-2	47.57	119.50	708.8	115.1	< 0.01	< 0.06	83.22	160.51	< 0.001	8.22	54.56	1.60	155.0
	ITS I3			736.9	126.4	< 0.01	< 0.06	104.59	143.40	< 0.001	9.46	54.26	1.77	178.7
Run 3	I1-3	47.70	167.03	638.4	97.7	< 0.01	< 0.06	100.99	no sample	< 0.001	15.54	69.60	no sample	227.8
	I2-3	47.85	167.35	668.7	101.5	< 0.01	< 0.06	103.43	182.20	< 0.001	14.51	48.67	1.76	187.8
	ITS I4			854.9	123.5	< 0.01	< 0.06	87.82	20.60	< 0.001	7.88	49.70	0.93	184.7
Run 4	I1-4	47.45	214.48	861.4	118.0	< 0.01	< 0.06	102.98	no sample	< 0.001	14.98	96.00	no sample	242.8
	I2-4	47.47	214.82	917.2	130.5	< 0.01	< 0.06	64.37	30.43	< 0.001	18.80	70.21	3.04	178.6
	ITS I5			909.7	130.9	< 0.01	< 0.06	73.04	missing	< 0.001	8.46	65.19	0.41	173.9
Run 5	I1-5	47.60	262.08	928.9	132.5	< 0.01	< 0.06	107.77	no sample	< 0.001	11.94	96.00	no sample	254.1
	I2-5	47.35	262.17	944.1	130.8	< 0.01	< 0.06	131.13	160.65	< 0.001	19.47	71.06	2.26	183.2

Table B-2. Molecular parameters collected during NOGEE experiment. Below detection limit is captured as bdl.

Iron NOGEEs	wet wt. extracted	DNA yield (ng)	dsr/gm ext	geo/gm ext.	mcr/gm ext.	dsr/ng DNA	geo/ng DNA	mcr/ng DNA
t_{o-1}	2.07	203.4	2.98E+05	6.95E+05	bdl	3.03E+03	7.08E+03	bdl
t_{o-2}	1.99	106.2	1.01E+05	2.74E+05	bdl	1.90E+03	5.14E+03	bdl
t_{o-3}	2.10	478.3	9.45E+05	1.80E+06	1.35E+03	4.15E+03	7.89E+03	5.93E+00
t_{o-4}	0.60	59.4	7.50E+04	1.49E+05	bdl	7.58E+02	1.51E+03	bdl
t_{o-5}	0.60	59.4	7.50E+04	1.49E+05	bdl	7.58E+02	1.51E+03	bdl
t_{o-6}	0.60	268.5	5.12E+05	2.28E+06	bdl	1.14E+03	5.09E+03	bdl
S1	0.24	598.5	6.69E+07	1.36E+07	4.97E+03	2.68E+04	5.45E+03	1.99E+00
S2	1.24	1055.2	1.31E+07	2.79E+06	3.54E+03	1.54E+04	3.28E+03	4.16E+00
I1	0.33	102.6	4.92E+05	3.86E+06	bdl	1.58E+03	1.24E+04	bdl
I2	0.33	108.3	9.92E+05	4.32E+06	bdl	3.02E+03	1.32E+04	bdl

VITA

Name: Andrea Melissa Howson

Professional Address: Marathon Oil Company,
5555 San Felipe
Houston, TX 77056

Email Address: andreahowson@gmail.com

Education: B.S., Geology, Texas A&M University, 2006

M.S., Geology, Texas A&M University, 2009